Blimp1 functions as a molecular switch to prevent production of inflammatory cytokines and loss of suppressor activity in RORγt$^+$Foxp3$^+$ Treg cells

Chihiro Ogawa[1,2,3], Rashmi Bankoti[1], Truc Nguyen[1], Nargess Hassanzadeh-Kiabi[1,4], Samantha Nadeau[1], Rebecca Porritt[1], Michael Couse[1], Xuemo Fan[5], Deepti Dhall[5], Gerald Eberl[6], Caspar Ohnmacht[6,7] and Gislâine A. Martins[1,2,3,8]

[1]F. Widjaja Foundation Inflammatory Bowel and Immunobiology Research Institute (IBIRI), Cedars-Sinai Medical Center (CSMC), Los Angeles, CA, [2]Depts. of Medicine, Division of Gastroenterology, and [3]Biomedical Sciences, Research Division of Immunology, CSMC, [4]CSMC Flow Cytometry Core, [5]Dept. of Pathology, [6]Institut Pasteur, Microenvironment and Immunity Unit, 75724 Paris, France, [7] Center of Allergy and Environment (ZAUM), Technische Universität and Helmholtz Zentrum München, Munich, Germany, [8]Lead Contact

*Corresponding Author: Gislâine A. Martins

Davis Res. Bldg, RM 4092, 110 N. George Burns Road,

Los Angeles, CA 90048, USA

Phone: (310) 423-0278, FAX: (310) 423-0224,

Email: martinsg@csmc.edu

Abstract:

Foxp3$^+$Treg cells are essential modulators of immune responses, but the molecular mechanisms underlying their phenotype and function are not fully understood. Here we show that the transcription factor Blimp1 is a crucial regulator of the RORγt$^+$ Foxp3$^+$ Treg cell subset function. The intrinsic expression of Blimp1 in these cells was required to prevent production of the inflammatory cytokine IL17 and loss of suppressive function in vivo. Mechanistically, Blimp1 acts as a direct repressor of the *Il17a/Il17f* genes and binding of Blimp1 at this locus is associated with increased accumulation of H3K27me3 and decreased H3K4me3, but unaltered binding of RORγt. However, in the absence of Blimp1 the *Il17a/Il17f* locus was activated, as shown by increased occupancy of the co-activator p300 and more abundant binding of the transcriptional regulator IRF4, which was required, along with RORγt for IL17A production in the absence of Blimp1. Using dual reporter mice, we also show that despite their sustained expression of Foxp3, Blimp1-deficient RORγt$^+$-IL17-producing Treg cells lose suppressor function in vivo, indicating that repression of IL17 expression by Blimp1 is a crucial requirement for this Treg subset function.

38

39 **Introduction:**

40 Regulatory T cells (Treg) are a subpopulation of T cells with the capability to suppress immune
41 responses (Fontenot et al., 2005; Kim et al., 2011) and are crucial for the maintenance of
42 immune homeostasis. The most well characterized Treg cell subpopulation is defined by the
43 expression of the transcription factor Foxp3 (Fontenot et al., 2005; Kim et al., 2011). Mutations
44 or deficiency of the *Foxp3* gene in mice and humans results in severe autoimmunity (Brunkow
45 et al., 2001) (Bennett et al., 2001). Foxp3^{+} Treg can develop in the thymus and in the periphery
46 (Apostolou et al., 2002; Fontenot et al., 2005) and recent studies support the notion that
47 functional specification in Treg subpopulations requires the expression of transcription factors
48 previously associated with the differentiation and function of effector CD4^{+} T-cell lineages
49 (Chaudhry and Rudensky, 2013; Levine et al., 2017; Wohlfert et al., 2011). Expression of these
50 Th cell lineage-specific transcription factors would drive the generation of effector Treg cells that
51 are specifically suited to regulate immune responses mediated by their corresponding
52 conventional effector CD4^{+} T-cell lineages. Thus, in the context of T helper type 1 (Th1)-
53 mediated inflammation, Tregs can upregulate expression of the Th1-specific transcription factor
54 T-bet, leading to the accumulation of Foxp3^{+} T-bet^{+} Tregs at sites of inflammation. T-bet^{+}
55 Foxp3^{+}Tregs were shown to be essential for control of type-1 inflammation (Levine et al., 2017).
56 Similarly, the Th2-associated transcription factor GATA3 was found to play an important role for
57 Treg function, and mice with GATA3-deficient Tregs have defects in peripheral homeostasis
58 caused by impaired Tregs suppressive function (Wohlfert et al., 2011). In addition, Treg-specific
59 deletion of the transcription factors IRF4 (interferon regulatory factor 4)(Zheng et al., 2009) or
60 STAT3 (signal transducer and activator of transcription 3)(Chaudhry et al., 2009) resulted in an
61 impaired regulation of Th2- and Th17-dominated immune responses, respectively. More recent
62 studies have identified a CD4^{+} Foxp3^{+} Treg cell population that simultaneously expresses the
63 transcription factor retinoic acid-related orphan receptor-γt (RORγt)(Lochner et al., 2008;

64 Ohnmacht, 2016; Ohnmacht et al., 2015; Sefik et al., 2015), initially described as crucial
65 requirement for development of Th17 cells. Foxp3$^+$RORγt$^+$ Treg cells were identified in both
66 mice and humans and are enriched in the intestinal mucosa, but can also be found in peripheral
67 organs such mesenteric lymph nodes and spleen (Ohnmacht, 2016; Ohnmacht et al., 2015;
68 Sefik et al., 2015). These cells lack expression of the transcription factor Helios, previously
69 associated with Foxp3$^+$ Treg cells from thymic origin and differ from the GATA$^+$ Foxp3$^+$ Treg
70 cells, which can also be isolated from the intestinal mucosa (Wohlfert et al., 2011) but are in
71 their majority Helios$^+$(Ohnmacht et al., 2015). Foxp3$^+$RORγt$^+$ Treg cells include the microbiota-
72 specific Treg cells and their frequency is greatly diminished in germ free mice or by treatment of
73 SPF mice with antibiotics (Ohnmacht, 2016; Ohnmacht et al., 2015; Sefik et al., 2015). This
74 Treg subpopulation expresses the regulatory cytokine IL10 and other molecules associated with
75 Foxp3$^+$ Treg cell function, such as ICOS, CTLA-4, CD39, and CD73 (Ohnmacht, 2016;
76 Ohnmacht et al., 2015). Despite their expression of RORγt and other genes associated with the
77 Th17 program, Foxp3$^+$RORγt$^+$ Treg cells do not produce IL17 (Lochner et al., 2008; Sefik et al.,
78 2015) and have potent suppressor function, but the mechanisms underlying their phenotype are
79 poorly understood.

80 B-lymphocyte-induced maturation protein-1 (Blimp1/PRDI-BFI) is a transcription factor
81 expressed in several hematopoietic lineages, including lymphocytes and myeloid cells (Linterman
82 et al., 2011; Martins and Calame, 2008). Blimp1 directly regulates the expression of genes
83 associated with T cell effector function, including cytokines (Cimmino et al., 2008; Martins et al.,
84 2008; Salehi et al., 2012). Blimp1 is highly expressed in a subset of Foxp3$^+$ Treg cells and it is
85 required for IL10 expression in these cells (Cretney et al., 2011; Martins et al., 2006) as well as
86 in Foxp3$^-$(Heinemann et al., 2014; Iwasaki et al., 2013; Montes de Oca et al., 2016; Neumann et
87 al., 2014; Parish et al., 2014) T cells, thus playing non-redundant roles in the function of both
88 effector (Teff) and regulatory (Treg) cells. In line with these findings, mice with T cell-specific

89 (CD4^{cre} or proximal LCK^{cre}-mediated) deletion of Blimp1 spontaneously develop chronic intestinal
90 inflammation (Martins et al., 2008; Martins et al., 2006; Salehi et al., 2012). However, Foxp3^{+}Treg
91 cell-specific deletion of Blimp1 leads to only mild intestinal inflammation associated with enhanced
92 production of IL10 by Foxp3^{-} T effector cells (Bankoti et al., 2017), indicating differential
93 requirements for Blimp1 in Foxp3^{+} and Foxp3^{-} T cells. The notion that Blimp1 plays differential
94 roles in Foxp3^{+} and Foxp3^{-} CD4^{+} T cells is also supported by the observation that Blimp1 regulates
95 a substantial amount of unique target genes in each cell type (Bankoti et al., 2017), however
96 intrinsic studies of Blimp1's role in Foxp3^{+} Treg cells have been somewhat hindered by the fact
97 that under homeostatic conditions, only a small fraction of Foxp3^{+} Treg cells express Blimp1
98 (Bankoti et al., 2017; Cretney et al., 2011).

99 In this study, we have further investigated the role of Blimp1 in Foxp3^{+} Treg cells and
100 report that Blimp1 expression in Foxp3^{+} Treg cells greatly overlaps with the expression of the
101 Th17-associated transcription factor RORγt, which defines a subset of microbiome-specific
102 Foxp3^{+} Helios^{-}Treg cells present under homeostatic conditions in mice and humans (Ohnmacht
103 et al., 2015; Sefik et al., 2015). We show that the expression of Blimp1 in this RORγt^{+}Foxp3^{+} Treg
104 cell subset is required and sufficient to repress expression of Th17-associated inflammatory
105 cytokines in an IL-10-independent manner. Using a dual reporter mice system, we show that
106 Blimp-1-deficient IL17-producing Foxp3^{+} Treg cells lose suppressor activity in vivo but are not
107 sufficient to cause inflammation in an experimental model of colitis. Our findings also reveal that
108 specific binding of Blimp1 to regions upstream of the *Il17a* and *Il17f* genes in wild-type Foxp3^{+}Treg
109 cells is associated with changes in the chromatin structure, including increased accumulation of
110 H3K27me3 and decreased accumulation of H3K4me3, histone modification markers associated
111 with the repression and activation respectively of the *Il17a and Il17f* genes in CD4^{+}T cells (Wei et
112 al., 2009). Lack of Blimp1 expression and the chromatin changes associated with it did not
113 interfere with binding of RORγt, but was associated with increased binding of the co-activator

114 p300 and of the transcription factor IRF4, which was required for RORγt-mediated induction of
115 the *Il17* locus in the absence of Blimp1. Thus, RORγt^{+} Foxp3^{+} microbiome-specific Treg cells rely
116 on Blimp1 to suppress production of Th17-associated cytokines and maintain their regulatory
117 function.
118
119 **Results:**
120 **Blimp-1 is preferentially expressed in RORγt^{+}Helios^{-} Foxp3^{+}Treg cells.**
121 Previous studies have shown that Blimp-1 is highly expressed in both murine and human Foxp3^{+}
122 Treg cells (Bankoti et al., 2017; Cretney et al., 2011; Ward-Hartstonge et al., 2017). To further
123 characterize Blimp1-expressing Foxp3^{+} Treg cells under homeostatic conditions we used dual
124 reporter mice (Foxp3^{RFP}/Blimp1^{YFP}) to isolate Foxp3^{+}Blimp-1^{+} and Foxp3^{+}Blimp1^{-} Treg cells and
125 evaluated the expression of several transcription factors previously associated with effector T cell
126 function. We found that expression of the Th17-associated transcription factor RORγt mRNA was
127 upregulated in Blimp1^{+}Foxp3^{+}Treg cells in comparison with Blimp1^{-}Foxp3^{+}Treg cells
128 (supplemental Fig. 1A). RORγt^{+}Foxp3^{+} Treg cells were recently described as peripherally-induced
129 microbiome-specific, Helios^{-} Foxp3^{+}Treg cells that are required to control effector responses in
130 the intestinal mucosa (Lochner et al., 2008; Ohnmacht, 2016; Ohnmacht et al., 2015; Sefik et al.,
131 2015). To confirm that Blimp1 was preferentially expressed in this Foxp3^{+}Treg subset, we
132 compared Blimp1 mRNA expression in Foxp3^{+}RORγt^{+}Helios^{-} and Foxp3^{+}RORγt^{-}Helios^{-}Treg cells
133 isolated from naïve mice. As shown in Fig. 1A, expression of Blimp1 mRNA (as reported by YFP)
134 under homeostatic conditions was consistently higher in Foxp3^{+}RORγt^{+}Helios^{-} than in
135 Foxp3^{+}RORγt^{-}Helios^{+} cells from both, the large intestines lamina propria (LI-LP) and mesenteric
136 lymph nodes (MLN). In addition, analysis of Blimp1 mRNA expression in RORγt^{+}Foxp3^{+} and
137 RORγt^{-}Foxp3^{+} Treg cells sort-purified from the intestinal mucosa of Foxp3 and RORγt dual
138 reporter mice showed preferential expression of Blimp1 in RORγt^{+}Foxp3^{+} Treg cells (Fig. 1B).

139 Conversely, expression of the transcription factor Bcl6 mRNA, which is directly suppressed by
140 Blimp1 (Cimmino et al., 2008) was less abundant in RORγt$^+$ Treg cells (Supplemental Fig. 1B).
141
142 **2. Expression of Blimp1 in Foxp3$^+$RORγT$^+$ Treg cells is required to repress IL17 expression**.
143 To further investigate Blimp1's role in RORγt$^+$Foxp3$^+$ Treg cells, we used *PRDM1*$^{F/F}$ mice crossed
144 with Foxp3$^{YFP\text{-}CRE}$ mice in which Blimp1 is specifically deleted in Foxp3$^+$T$_{reg}$ cells(Bankoti et al.,
145 2017). Evaluation of Foxp3$^+$RORγt$^+$ Treg cells in *Prdm11*$^{F/F}$/Foxp3$^{YFP\text{-}CRE+}$mice and their littermate
146 controls (*Prdm1*$^{+/+}$Foxp3$^{YFP\text{-}CRE+}$) showed that the frequency of RORγt$^+$ Foxp3$^+$ Treg cells was
147 elevated in mice with Blimp1-deficient Treg cells, whereas the frequency of RORγt$^-$GATA-3$^+$
148 Foxp3$^+$ Treg cells was unaltered (Sup. Fig. 1C). Analysis of cytokine expression upon in vitro
149 stimulation revealed that Blimp1-deficient RORγt$^+$ Foxp3$^+$ Treg cells produce the inflammatory
150 cytokine IL17A (Fig. 1C) but not IFNγ or IL-4 (data not shown). Similar results were obtained when
151 we evaluated IL17A expression in mice with T cell-specific deletion of *Prdm1* (*Prdm1*$^{F/F}$/CD4^{CRE+})
152 crossed with Foxp3^{RFP} and IL17^{GFP} double reporter mice, in which we detected IL17A-expressing
153 RORγt$^+$Foxp3$^+$ cells in the MLN and LI-LP in addition to the lungs (Supplemental. Fig. 2A), which
154 have also been previously show to contain RORgt$^+$Foxp3$^+$ Treg cells (Lochner et al., 2008). Of
155 note, most the IL17F-expressing RORγt$^+$Foxp3$^+$ Treg cells were also IL17A-positive
156 (Supplemental. Fig. 2B), indicating that both *Il17a* and *Il1f* genes were activated in these cells.
157 These findings were also reproduced in *Prdm1*$^{F/F}$/CD4^{CRE+}mice devoid of any reporter gene, in
158 which simultaneous staining of Foxp3 and IL17A proteins revealed significant expression of IL17A
159 by Blimp-1-deficient Foxp3$^+$ Treg cells (Supplemental Fig.2C). Moreover, in comparison to
160 Blimp1-sufficient, Blimp1-deficient sorted Foxp3$^+$ Treg cells secreted measurable amounts of
161 IL17A and, as expected from previous studies implicating Blimp1 as a positive regulator of IL10
162 expression in Foxp3$^+$ Treg cells (Cretney et al., 2011; Martins et al., 2006), Blimp1-deficient
163 Foxp3$^+$ Treg cells produced reduced amounts of IL10 upon in vitro TCR stimulation (Supplemental

164 Fig. 2D). Of note, all the IL17A-producing Foxp3^{+} Treg cells in the *Prdm1*$^{F/F}$Foxp3$^{YFP\text{-}CRE+}$ mice
165 expressed RORγt and co-expressed the transcription factor IRF4 (Fig. 1D), which has been
166 previously shown to be required for both Treg cell function (Zheng et al., 2009) and IL17
167 production in Th17 cells (Brustle et al., 2007; Ciofani et al., 2012) .However, lack of Blimp-1 did
168 not alter the amounts of RORγt or IRF4 protein expressed by Foxp3^{+} Treg cells on a per cells
169 basis (Fig. 1D), indicating that Blimp1 does not regulate the expression of *Rorc* or *Irf4* in these
170 cells. In line with that, expression of RORγt and IRF4 mRNA were similar in Blimp-1 sufficient and
171 Blimp1-deficient Foxp3^{+}Treg cells (Supplemental Fig. 2E). To further confirm that production of
172 IL17A by a subset of Blimp1-deficient Foxp3^{+} Treg cells is a cell-intrinsic effect, we next evaluated
173 female *Prdm1*$^{F/F}$Foxp3$^{YFP\text{-}CRE+}$ mice which allowed the comparison of Blimp1-sufficient and
174 Blimp1-deficient Foxp3^{+}Treg cells in the same animal. We found that even in the presence of
175 Blimp1-sufficient Treg cells, Blimp1-deficient CD4^{+}Foxp3^{YFP+} cells produced IL17A protein
176 whereas expression of IL10 was diminished (Fig. 1E). In addition, although Blimp1-deficient Treg
177 cells expressed Foxp3 and RORγt mRNA at levels comparable to the control cells, they expressed
178 substantial amounts of IL17A and IL17F mRNA (Fig. 1F and Supplemental Fig. 2F), thus
179 confirming that Blimp1-deficient RORγt^{+}T$_{reg}$ cells are intrinsically prone to produce Th17-
180 associated cytokines. Of note, in comparison to IL17-negative counterparts, IL17-producing
181 Blimp1-deficient Foxp3^{+}RORγt^{+} Treg cells expressed higher levels of activation markers and other
182 surface molecules known to be associated with Treg cell effector phenotype (Supplemental Fig.
183 3), which is in line with previous observations that Blimp1 is preferentially expressed in effector
184 Treg cells (Bankoti et al., 2017; Cretney et al., 2011; Dias et al., 2017).
185 We also found that addition of recombinant IL10 to Blimp1-sufficient and deficient Foxp3^{+} Treg
186 cells cultured in vitro in the presence of inflammatory cytokines did not abrogate production of
187 IL17A or altered RORγt expression (Supplemental Fig. 4A-B) in the absence of Blimp1, indicating
188 IL17A expression by these cells is not a secondary effect of the diminished IL10 expression. This

189 was further confirmed by the observation that in comparison with wild type Foxp3$^+$ T_{reg} cells, IL10-
190 deficient Foxp3$^+$ T_{reg} have only a small, non-significant increase in IL17A expression
191 (Supplemental Fig. 4C).
192 We next sought to determine if the Foxp3$^+$RORγt$^+$ Treg cells that produce IL17A in Blimp1CKO
193 mice were susceptible to depletion of the microbiome, as previously observed for
194 RORγt$^+$Foxp3$^+$Treg cells (Ohnmacht et al., 2015). We found that treatment of Blimp-1CKO mice
195 with a combination of antibiotics previously shown to eliminate most of the intestinal microbiome
196 and to reduce the numbers of RORγt$^+$ Foxp3$^+$ Treg cells, led to a significant decrease in IL17-
197 producing Blimp1-deficient Foxp3$^+$Treg cells (Fig. 1G). Thus, expression of Blimp1 in RORγt$^+$
198 Foxp3$^+$Teg cells is intrinsically required to prevent production of Th17-associated inflammatory
199 cytokines, and Blimp-1-deficient RORγt$^+$ IL17-producing Treg cells are reduced upon disruption
200 of the intestinal microbiota by antibiotic treatment.
201
202 **3. Blimp1 binding to the *Il17a* and *Il17f* genes locus results in diminished accessibility of**
203 **chromatin.**
204 The observation that Blimp1-deficient Foxp3$^+$Treg cells produce T_{h17}-associated cytokines but do
205 not have increased expression of Th17-inducing transcription factors along with our previous
206 observation that Blimp1 could directly bind to a regulatory region in the *Il17a* gene in T_{h2} cells
207 (Salehi et al., 2012) indicated that Blimp1 could function as a direct suppressor of the *Il17a/Il17f*
208 genes in Treg cells. To address this, we first determined if enforced expression of Blimp1 in
209 Blimp1-deficient Foxp3$^+$ Treg cells was sufficient to abrogate expression of IL17. We found that,
210 differently from observed in in vitro-differentiated Th17 cells, retroviral-driven expression of Blimp1
211 led to significant repression of IL17 in Blimp1CKO Treg cells (Fig. 2A). We next performed ChIP
212 analysis of Blimp1-suficient Foxp3^{GFP+} cells stimulated *in vitro* in conditions that induced *Il17a and*
213 *Il17f* mRNA expression. We found that Blimp1 directly binds to a previously identified site located

214 downstream of conserved non-coding sequence 2 (CNS2) upstream of the *Il17a* gene
215 transcription start site and strongly binds to two other previously unidentified consensus sites
216 located at the *Il17a* promoter and at the CNS7 region located upstream of the *Il17f* promoter but
217 not to another region containing Blimp1 consensus binding site (*Il17a* intron I) or to a non-related
218 region in the same locus (Fig. 2B). Binding of Blimp1 at these sites in Treg cells was significantly
219 higher than in pathogenic Th17 cells, in which Blimp1 is expressed at very low levels (Bankoti et
220 al., 2017), but was reported to bind to similar regions of the *Il17* locus (Jain et al., 2016). Thus,
221 Blimp1 directly binds to conserved regulatory regions at the *Il17a* and *Il17f* genes and could
222 directly repress the expression of this locus in a subset of Foxp3^{+}Treg cells. To determine whether
223 recruitment of Blimp1 to the *Il17a and Il17f* locus in Treg cells would correlate with changes in
224 histone modifications associated with the repression or activation of the locus, we evaluated the
225 enrichment of Histone 3 trimethylated at Lys9 (H3K9me3), which is associated with activation of
226 the *Il17a and Il17f* genes in Th17 cells and H3K27me3, associated with repression of these genes
227 in other T cell subsets (Bankoti et al., 2017; Kim and Belza, 2017). We found that recruitment of
228 Blimp1 is associated with increased H3K4me3 in three different regions of the *Il17a* and *Il17f*
229 locus including CNS2, *Il17a* intron 1 and CNS7 (Fig. 2C). Importantly, lack of Blimp1 resulted in
230 significantly decreased deposition of H3K27me3 specifically at CNS7 but not at CNS2 or *Il17a*
231 Intron I, indicating that Blimp1 binding at the CNS7 region could be required for H3K27me3
232 accumulation and most likely suppression of *Il17a* and *Il17f* transcription. This is further supported
233 by the observation that binding of p300, a histone acetyltransferase that usually marks active
234 transcription in regulatory domains, was also significantly increased at the CNS7 region of the
235 *Il17* locus in Blimp1-deficient Foxp3^{+}Treg in comparison to Blimp1-sufficient Treg cells (Figure
236 2D). Of note, the amounts of p300 bound at this region in Blimp1-deficient Treg cells were similar
237 to the observed in wild type pathogenic Th17 cells, in which the *Il17* locus is fully active.
238 Using a luciferase reporter construct containing the CNS7 region upstream of the *Il17a*
239 promoter region, we find that the CNS7 region can function as an enhancer for the *Il17a* promoter

240 and this activity is abrogated in the presence of a full-length but not of a truncated Blimp1 construct
241 lacking a DNA-binding domain (Fig. 2E). Thus, binding of Blimp1 at the *Il17a/Il17f* CNS7 region
242 help to prevent/control locus activation and therefore the production of Th17-associated cytokine
243 by Foxp3^{+}Treg cells
244
245 **4. Increased binding of IRF4 at the *Il17* locus promotes expression of T_{h17}-associated**
246 **cytokines in Blimp1-deficient Treg cells.**
247 The activation and increased accessibility of the *Il17a/Il17f* locus resulting from lack of Blimp1 in
248 Treg cells, led us to interrogate if in the absence of Blimp1 binding of RORγt could be facilitated,
249 and therefore mediate the increased *Il17a* and *Il17f* transcription observed in Blimp1-deficient
250 Treg cells. We thus performed ChIP of RORγt in Blimp1-sufficient and deficient Treg cells, but
251 found no significant increase in RORγt binding at the *Il17a/f* locus in the absence of Blimp1 (Fig.
252 3A), indicating that Blimp1-mediated repression of the *Il17a/Il17f* genes in Treg cells is not
253 achieved by impairment of RORγt binding to the locus. However, RORγt expression was required
254 for the expression of IL17 by Blimp1-deficient Treg cells, as IL17 expression was significantly
255 inhibited in Blimp-1 and RORγt double knock out cells (Fig. 3B).
256 We next interrogated if IRF4, which is highly expressed in Treg cells and one of the pioneer
257 transcription factors required for Th17 specification (Ciofani et al., 2012) could be involved in
258 regulating activation of the *Il17* locus in Blimp1-deficient Treg cells. Although IRF4 expression
259 levels were similar in Blimp1-sufficient and deficient Treg cells (Fig. 1D and Supplemental Fig.
260 2E) ChIP assays revealed that Blimp1-deficient cells had a significant increase in IRF4 binding at
261 the *Il17* CNS7 region (Fig. 3C). Binding of IRF4 at the *Il10* intron 1, a region previously shown to
262 be bound by IRF4 in Treg was not altered in Blimp1-deficient Treg cells. Thus, lack of Blimp1 led
263 to a specific increase in IRF4 binding at the *Il17* locus.

264 To determine if increased binding of IRF4 to this locus could mediate the increased
265 transcription of *Il17a* and *Il17f* in Blimp1-deficient Treg cells, we used short interference RNA to
266 mediate silencing of IRF4 in Blimp1-deficient Treg cells and interrogate if IRF4 knock down could
267 interfere with IL17A expression in these cells. As shown in Fig. 3D, a reduction of approximately
268 50% in IRF4 expression resulted in significant decrease in IL17A expression, but unaltered IL10
269 expression in Blimp1-deficient Treg cells, indicating that the production of IL17A in these cells is
270 at least partially mediated by IRF4, and IRF4 binding is increased at the *Il17* locus in the absence
271 of Blimp1.
272
273 **5. Blimp1-deficient IL17-producing Foxp3^{+} T$_{reg}$ cells lose suppressor activity in vivo.**
274 We and others have previously shown that despite their impaired IL10 production, peripheral
275 Blimp1-deficient T$_{reg}$ cells preserve their suppressive function *in vitro* and in some circumstances
276 in vivo as well (Martins et al, 2006; (Crotty et al., 2010; Kim et al., 2007). However, these results
277 might have been confounded by the fact that Blimp1-deficient Foxp3^{+} Treg cells are a
278 heterogenous population in which only the RORγt-expressing cells produce IL17A. To specifically
279 test the function of the IL17A-producing Blimp1-deficient Foxp3^{+} Treg cells, we used Foxp3^{RFP}
280 and IL17A^{GFP} double reporter *Prdm1*$^{F/F}$/CD4^{CRE+} mice to sort IL17A^{GFP}-producing and
281 nonproducing Blimp1-deficient Foxp3^{+} Treg cells (Supplemental Fig. 5A) and evaluate their
282 function on a T cell adoptive transfer colitis induction model. As shown in Fig. 4, transfer of allotype
283 marked (CD45.1^{+}) naïve (CD45RB^{hi}) CD4^{+} T cells to Rag1$^{-/-}$ mice, led to inflammation in the colon,
284 associated with impaired body weight gain (Fig. 4A), colon shortening (Fig. 4B) and histological
285 changes (Fig. 4C). Co-transfer of Blimp-1-deficient, Foxp3^{RFP+} IL17A^{GFP-} single positive cells
286 prevent colitis development, whereas Blimp-1-deficient Foxp3^{RPF+} IL17A^{GFP+}- double positive Treg
287 cells failed to prevent colitis induction in this model (Fig. 4A-C). Importantly, although expression
288 of expression of IL10 is reduced in Blimp1-deficient Foxp3^{+}Treg in comparison to wild type cells,
289 expression of IL10 in Blimp1-deficient Treg cells did not preferentially segregated with expression

290 of IL17 (Supplemental Fig. 4B). Similarly, expression of CTLA-4, ICOS (Supplemental. Fig. 5C)
291 and GITR (Supplemental Fig 5D) were comparable in IL17^{+} and IL17^{-}-Blimp1-deficient Treg cells.
292 In addition, although we detected significant loss of Foxp3 expression upon transfer of both
293 Foxp3^{+}IL17A-producing and non-producing Treg cells, expression of Foxp3 in the recovered cells
294 (CD45.2^{+}) was about three times higher in IL17-producing cells (Fig. 4D). Importantly, the
295 numbers of recovered CD45.1^{+} cells (originating from adoptively transferred naïve CD4^{+} T cells)
296 were consistently decreased in the intestinal mucosa and spleens of mice that also received
297 IL17A-non-producing Foxp3^{+} Treg cells, whereas mice co-transferred with IL17-producing
298 Foxp3^{+}Treg cells had variable numbers of recovered CD45.1^{+} cells, which in average were not
299 significantly different from the observed in the other experimental groups. Together, these
300 observations suggest that IL17-expressing Foxp3^{+} Treg cells might be less efficient in
301 suppressing effector T cell expansion in this model. Of note, Foxp3^{+}IL17A-producing Treg cells
302 retained IL17A production upon transfer (Fig. 4E), which resulted in higher secretion of IL17A by
303 intestinal lamina propria cells from mice adoptively co-transferred with these cells, in comparison
304 to mice that only received naïve cells or naïve cells co-transferred with Foxp3^{+}IL17A non-
305 producing cells (Fig. 4F). Despite their impaired suppressor activity, Blimp1-deficient IL17-
306 producing Treg cells were not sufficient to cause intestinal inflammation when compared with in
307 vitro differentiated pTh17 cells on an adoptive cell transfer model of colitis (Supplemental Fig. 6).
308 Thus, expression of Blimp1 in RORγt^{+} microbiome-specific Foxp3^{+} Treg cells is required to
309 prevent expression of Th17-associated cytokines and to maintain suppressive function in vivo.
310

311 **Discussion:**

312 Our studies described here reveal a novel, unexpected role for the transcription factor
313 Blimp1 in controlling key functional aspects of a specific Foxp3$^+$ Treg cell subset. We show that
314 Blimp-1 is preferentially expressed by a RORγt$^+$ Foxp3$^+$Treg subset found under homeostatic
315 conditions in mice and men, and the intrinsic expression of Blimp1 in these cells is required to
316 restrain production of T_{h17}-associated cytokines and maintain their suppressive function in vivo.
317 Blimp1 functions as a direct repressor of the *Il17a* and *Il17f* locus in Foxp3$^+$Treg cells and its direct
318 binding to this locus alters chromatin structure and restricts binding of the T_{h17}-associated factor
319 IRF4, which is required, along with RORγt for IL17-production in Blimp1-deficient Foxp3$^+$ cells
320 (Supplemental Fig. 7). These findings uncover a new aspect of Blimp1's role in Foxp3$^+$ Treg cell
321 biology and sheds light on the intricate mechanisms that regulate T_{reg} cell phenotypic stability.

322 RORγt$^+$-microbiome-specific Foxp3$^+$Treg cells were recently described as an important
323 component of the NRP-1$^-$Helios$^-$Foxp3$^+$ Treg cell pool that controls homeostasis in the intestinal
324 mucosa, including control of Th1, Th2 and Th17 effector responses (Lochner et al., 2008;
325 Ohnmacht, 2016; Sefik et al., 2015). These cells seem to develop in response to pathobionts (Xu
326 et al., 2018) and also depend on the transcription factor cMaf for their differentiation and function
327 (Wheaton et al., 2017; Xu et al., 2018). Expression of the Th17-associated transcription factor
328 RORγt by this Treg subset was shown to be required for their homeostasis such that Foxp3-
329 specific deletion of RORγt resulted in substantial decrease in the numbers of Foxp3$^+$Helios$^-$ Treg
330 cells in the intestinal mucosa and, at least in one model, led to spontaneous increase in Th17
331 responses (Sefik et al., 2015). Despite their constitutive expression of RORγt, under homeostatic
332 conditions these cells do not produce IL17 (Sefik et al., 2015) and have potent regulatory function,
333 associated with the expression of IL10 and CTLA-4 (Ohnmacht, 2016; Ohnmacht et al., 2015;
334 Sefik et al., 2015). Of note, these RORγt$^+$Foxp3$^+$ T reg cells are found under homeostatic
335 conditions and differ a from a recently described subset of Foxp3$^+$RORγt$^+$Helios$^+$ Treg cells that

336 appear to develop or expand from a population of antigen-specific thymic-derived Foxp3$^+$ Treg
337 cells upon induction of inflammation in mice (Kim et al., 2017). The latter is thought to be specific
338 to auto-antigens and don't seem to be present under homeostatic conditions.

339 Here we show that expression of Blimp1 is required to prevent production of Th17-
340 associated cytokines in Helios$^-$RORγt$^+$Foxp3$^+$ Treg cells that are found under homeostatic
341 conditions and enriched at the intestinal mucosa. Blimp1-deficient RORγt$^+$Foxp3$^+$ Treg cells
342 produce IL17A, F and although these cells are not sufficient to cause inflammation, they have
343 impaired suppressive function in vivo. Importantly, Blimp1-deficient RORγt$^+$ Foxp3$^+$Treg cells
344 produced IL17A in the presence of exogenous IL10 *in vitro*, and IL10-deficient Treg cells do not
345 produce significant amounts of IL17A. Thus, acquisition of inflammatory properties by these cells
346 is not a secondary effect of the impairment in IL10 production associated with lack of Blimp1
347 (Cretney et al., 2011; Crotty et al., 2010). Moreover, we show that IL17A production by Blimp1-
348 deficient Foxp3$^+$ RORγt$^+$ Treg cells does not preferentially segregate with lower expression of
349 molecules required for Treg suppression function (Josefowicz et al., 2012), including IL10, CTLA-
350 4, GITR and ICOS. Although we have not directly specifically addressed TCR specificity in the
351 IL17-producing Blimp1-deficient Foxp3$^+$RORγt$^+$ Treg cells, we find that antibiotic treatment greatly
352 reduces the number of these cells in Blimp1-deficient mice, suggesting that these cells are
353 microbiome dependent, as previously shown for RORγt$^+$ Foxp3$^+$ Treg cells.

354 We also show that IL17A-producing Blimp1-deficient, RORγt$^+$ Treg cells maintain
355 expression of Foxp3 protein, suggesting that these cells are not immediately transitioning from
356 Treg into Th17 cells, a phenotype observed in some inflammatory conditions (Rubtsov et al.,
357 2008). These observations would indicate that other mechanisms in addition to direct action of
358 Foxp3 are used in Treg cells to repress production of inflammatory cytokines. Of interest, Blimp1
359 expression can be induced in Treg cells by inflammatory stimuli, such IL6 [(Cretney et al., 2011)
360 and data not shown], possibly as a negative feedback to protect Treg cells from turning into

361 pathogenic cells. In addition, Foxp3 could also function as a direct inducer of Blimp1 expression
362 in Treg, as *Prdm1* was previously shown to be a direct target of Foxp3 in these cells (Zheng et
363 al., 2007). In line with this, "ex-T_{reg}" cells that lost Foxp3 expression and produce IL17 under
364 chronic inflammatory conditions in a RA model have diminished expression of Blimp1 (Rubtsov
365 et al., 2008).

366 The mechanisms underlying the repression of the production of T_{h17}-associated cytokines
367 by Blimp1 in Foxp3$^+$ Treg cells do not involve repression of the expression of known Th17-
368 promoting transcription factors (Zhou and Littman, 2009) such as RORγt, RORα , B-ATF, IRF4,
369 or Runx, as we found no significant differences in the expression of these factors in Ctrl and CKO
370 Foxp3$^+$ cells. These data, in addition to our finding that Blimp1 can specifically bind to regulatory
371 regions in the *Il17a* and *Il17f* locus and its binding to the CNS7 region can suppress *Il17a* promoter
372 activity, points to a direct role for Blimp1 in repressing this locus in Treg cells. This is further
373 supported by the observation that Blimp1 binding is associated with decreased deposition of the
374 permissive chromatin modification markers H3K4me3. In addition, Blimp1-deficient Treg had
375 decreased levels of H3K27me3 at the CNS7 region, which is in close proximity to a region
376 previously shown to be highly active in Th17 but repressed in Treg cells (Wei et al, 2009) (Bankoti
377 et al., 2017) (Bankoti et al., 2017) (Bankoti et al., 2017), thus suggesting an important role for this
378 region in regulating expression of *Il17a* and *Il17f*. Importantly, in addition to the chromatin changes
379 at the *Il17a* and *Il17f* locus associated with the absence of Blimp1 in Foxp3$^+$ Treg cells, Blimp-1-
380 deficiency was also associated with increased binding of the co-activator p300, which occupancy
381 at the CNS7 region in Blimp-1-deficient T_{reg} cells reached similar levels to those observed in
382 pathogenic (p)Th17 cells, in which the *Il17* locus is fully active, further confirming activation of this
383 locus in Blimp1-deficient Foxp3$^+$ Treg cells.

384 Although we cannot establish direct causality between binding of Blimp1 at the *Il17a* and
385 *Il17f* locus and the histone modifications discussed above, it is intriguing that CNS7 is the only
386 region with significant changes in H3K27me3 accumulation in Blimp1-deficient Treg cells. The

387 other two locus regions (CNS2 and *Il17a* intron I) with increased H3K4me3 but no significant
388 H3K27me3 changes in CKO cells either lack Blimp1 binding sites (CNS2) or have a consensus
389 binding site that is not enriched for Blimp1 (*Il17a* Intron I). Thus, it seems likely that direct binding
390 of Blimp1 is required for the deposition of this specific repression marker. Trimethylation on
391 H3K27 is added by the Polycomb repressive complex (PRC) 2, which contains the
392 methyltransferase enhancer of Zeste homolog 2 (EZH2) which contains a SET domain
393 responsible for H3K27me3 (Ahn et al., 2017). Targeting of EZH2 and PRC2 to specific loci is
394 thought to be mediated by a variety of sequence elements including CpG islands, conserved
395 elements and the presence of specific transcription factors binding motifs (Yamanaka et al.,
396 2017). Thus, it is conceivable that Blimp1 binding could be involved in targeting EZH2/PRC2 to
397 the *Il17a* and *Il17f* locus, but this remains to be tested.

398 Of note, the chromatin changes associated with Blimp1 deficiency did not alter binding of
399 RORγt to the *il17af* locus. This suggests that the physical interaction between RORγt and Foxp3,
400 which has been previously reported to inhibit RORγt- mediated transcription of the *il17a/f* locus in
401 Treg cells (Ichiyama et al., 2008; Zhou et al., 2008) is preserved in Blimp1-deficient Treg cells.
402 Instead, we found that in the absence of Blimp1, IRF4 occupancy of the *Il17* locus CNS7 region
403 was increased. IRF4 knockdown led to significant reduction of IL17A production by Blimp1-
404 deficient Foxp3$^+$ Treg cells, indicating a requirement for IRF4 in mediating production of the Th17-
405 associated cytokines in Blimp1-deficient Treg cells. In addition, genetically ablation of RORγt led
406 to abrogation of IL17A expression in these cells. Together these observations support a model
407 by which IRF4 function in RORγt$^+$ Treg cells can be, is modulated by Blimp1, such that in the
408 absence of Blimp1 IRF4 is more prone to bind to the locus and potentially facilitate RORγt-
409 induced IL17 expression (Supplemental Figure 7).

410 Our finding that Blimp1 functions as a suppressor of the *Il17a* locus in Foxp3$^+$ Treg cells
411 might seem at odds with a recent study in which Blimp1 was implicated as an activator of the *Il17*

412 locus in pTh17 cells(Jain et al., 2016). In that study, in vivo differentiated pTh17 cells were shown
413 to have a small reduction in IL17A expression in the absence of Blimp1 but the expression IL17A
414 was not evaluated in Blimp1-deficient Foxp3^{+} cells. In the same study Blimp1 was shown by ChIP-
415 seq to be bound to different regions of the *Il17a/f* locus, including the CNS7 region in pTh17 cells.
416 However, in our experiments side-by-side comparison of Blimp1 occupancy of the *Il17* locus in
417 nTreg and pTh17 cells by qPCR- ChIP detected significant binding of Blimp1 to the CNS7 (and
418 two other *Il17* locus regions) in nTreg but not in pTh17 cells (Fig. 2B). It is possible that these
419 conflicting results could be explained by technical differences (e.g. use of different antibodies,
420 different ChIP methodologies).

421 An alternative explanation could be that Blimp1 does have opposite functions in the same
422 locus in nTreg and pTh17 cells, functioning as a repressor in the former and as an activator in the
423 later. Previous studies indicate that Blimp1 function can be dose-dependent (Robertson et al.,
424 2007), and we find that that the amount of Blimp1 protein expression in pTh17 cells is significantly
425 lower than in nTreg (Bankoti et al., 2017). In addition, Blimp1 function could also depend on the
426 differential availability of co-factors in these cells types. This could also explain why enforced
427 expression of Blimp1 suppress the *il17a/f* locus in Treg but not in Th17 cells (Fig. 2 and (Salehi
428 et al., 2012).These possibilities remain to be investigated.

429 Overall, our results support the idea that Blimp1 is required to prevent the production of
430 Th17-associated cytokine in RORγt-expressing, microbiome-specific Foxp3^{+}Treg cells, by a
431 mechanism that involves direct regulation of the *Il17a/f* locus. In addition, our study provides
432 evidence that Foxp3^{+}Treg cells that acquire the capability to produce inflammatory cytokines have
433 impaired suppressor function in vivo. Together these findings shed new light in to the mechanisms
434 regulating Treg cell phenotypic stability and function.

435

436

437 **Methods:**

438 **Mice:** C57BL/6*Prdm1*$^{flox/flox}$, C57BL/6*Prdm1*$^{flox/floxCD4\text{-}Cre+}$ and *Prdm1*$^{+/+CD4\text{-}Cre+}$mice were previously
439 described (Crotty et al., 2010; Johnston et al., 2009). B6.SJL-^{PtprcaPep3b}/BoyJ (CD45.1^{+}), mice
440 expressing CRE recombinase and yellow fluorescent protein (YFP) under the control of Foxp3
441 promoter, Foxp3$^{YFP\text{-}CRE}$ (C57BL/6-*Foxp3*$^{tm4\ (YFP/cre)Ay}$ or Foxp3$^{YFP\text{-}CRE}$), mice expressing GFP under
442 control of the IL17 regulatory region (C57BL/6-*Il17a*^{tm1Bcgen}/J, or IL17A^{eGFP}), mice expressing red
443 fluorescent protein (RFP) under control of the Foxp3 promoter (C57BL/6-*Foxp3*^{tm1Flv}/J, or
444 Foxp3^{RFP}), mice with "floxed" *Rorc* alleles B6(Cg)-*Rorc*^{tm3Litt}/J or *Rorc*$^{flox/flox}$) and IL10$^{-/-}$ (B6.129P2-
445 *Il10*^{tm1Cgn}/J) mice were obtained from Jackson labs. Mice bearing a BAC transgene encoding YFP
446 under the control of Blimp1 regulatory elements (Blimp1^{YFP}mice) in which YFP expression
447 faithfully reports Blimp1 mRNA expression (Johnston et al., 2009; Salehi et al., 2012) were
448 obtained from Eric Meffre (Yale University) and bread to Foxp3^{RFP} mice to generated
449 Blimp1^{YFP}Foxp3^{RFP} dual reporter mice. Foxp3^{RFP} mice were also bred to ROR(γt)-GFP mice or
450 to IL17A^{eGFP} mice to generate Foxp3^{RFP}IL17^{GFP} or Foxp3-RFP/RORγt-GFP dual reporter mice
451 or to C57BL/6*Prdm1*$^{flox/flox}$ mice to generated *Prdm1*$^{flox/flox}$*Foxp3*^{RFP} mice. Foxp3$^{YFP\text{-}CRE}$ mice were
452 bred to C57BL/6*Prdm1*$^{flox/flox}$ mice to generate mice with Treg-specific deletion of Blimp1
453 (*Prdm1*$^{flox/flox}$/Foxp3$^{YFP\text{-}CRE}$ mice). *Prdm1*$^{flox/flox}$/Foxp3$^{YFP\text{-}CRE}$ mice were then bred to *Rorc*$^{flox/flox}$ mice
454 to generate mice with Treg-specific double deficiency of Blimp1 and Rorγt. IL10$^{-/-}$ mice were bred
455 with Foxp3^{GFP} to generate IL10KOFoxp3^{GFP}. All mice were bred and maintained in the CSMC SPF
456 animal barrier facility and handled in accordance with the institutional guidelines.

457

458 **Antibodies and reagents**: The following antibodies (all from Biolegend, San Diego, CA) were
459 used for cell surface or intracellular staining: Alexa Fluor (AF) 700-conjugated anti-TCRβ (clone
460 H57-597), APC-Cy7 or Pacific Blue (PB)-conjugated anti-CD4 (clone RM4-5), PB-, APC-Cy7 or
461 APC-conjugated anti-CD44 (clone IM7), AF700-conjugated anti-ICOS (clone C398.4), APC or

462 PE-conjugated anti-IL17A (TC11-18H10.1), and APC-conjugated anti-IFNγ (clone XMG1.2).
463 APC-conjugated anti-CD25 (clone PC61), PE and APC-conjugated anti-Foxp3 (clone FJK-16s)
464 eFluor 450-conjugated anti Helios (22F6), PE-conjugated anti IL10 (JES5-16E3), PE-conjugated
465 anti IRF4 (3E4), eFluor 450-conjugated anti-CD103 (clone 2E7), and PE-conjugated anti-RORγt
466 (clone AFKJS-9) from eBiosicences, Inc. (San Diego, CA). BV786 or BV421-conjugated anti
467 RORgt (Q31-378), BUV395-conjugated anti Gata3 (L50-823) and BV510-conjugated anti IL10
468 (JES5-16E3) from BD Biosciences (San Jose, CA). Rabbit anti-GFP antibody (catalog 600-402-
469 215 Rockland Immunochemicals, Gilbertsville, PA) was used to stain Blimp1^{YFP} and Foxp3^{GFP}
470 reporter cells when intracellular staining for Foxp3 was performed. Foxp3 staining was done
471 using eBioscience Foxp3 staining kit (catalog 42-1403) or BioLegend's FOXP3 Fix/Perm Buffer
472 Set (catalog 421403). Samples were acquired on a LSRII analyzer and FACSymphony (BD
473 Biosciences).FACS data was analyzed with FlowJo software (Treestar, Ashland OR).

474

475 **Antibiotic treatment:** Mice were treated for 6 wks with a cocktail of the following antibiotics in
476 their drinking water: 1mg/ml vancomycin (Gold Biotechnology, St. Louis, MO), 0.5mg/ml
477 metronidazole (Sigma-Aldrich, St. Louis, MO), 1mg/ml neomycin (Gold Biotechnology), 1mg/ml
478 ampicillin (Sigma-Aldrich), 0.5mg/ml Fluconazole (Sigma-Aldric) and 1.5% glucose (Sigma-
479 Aldric).

480

481 **Cytokine production measurement**: Cytokine production was measured in the supernatant of
482 cell culture using eBioscience kits (IL10; IL17A) per the manufacturer instructions. Cytokine-
483 expressing cells were detected by intracellular staining and flow cytometry analysis. For
484 Intracellular cytokine staining, single cell suspension from peripheral organs were stimulated
485 with plate-bound anti-CD3 (5 μg/ml; BioXcell, West Lebanon, NH) and anti-CD28 (2.5 μg/ml;
486 BioXcell) for 24 hrs or with PMA (2 ng/ml; Sigma-Aldrich) and Ionomycin (0.2 ng/ml; Sigma-

487 Aldrich) for 4 hrs. Brefeldin A (Sigma-Aldrich) was added in the last 6 or 2 hrs of incubation,
488 respectively. Cells were collected, surface stained and fixed with 4% paraformaldehyde followed
489 by staining of cytokines.

490 **In vitro T helper 17 differentiation**: Blimp1-deficient Th17 cells used for retroviral transduction
491 were stimulated as previously described (Salehi et al., 2012). pTh17 cells used for ChiP assays
492 were generated as previously described (Jain et al., 2016). To generated IL17^{GFP+} Th17 cells used
493 in the adoptive transfer colitis experiments, naïve (CD62L^{High}CD44^{Low}Foxp3^{RFP-}) were sorted from
494 IL-17A^{eGFP} Foxp3^{RFP} double report mice and cultured with irradiated antigen presenting cells (1:4
495 ratio), in the presence of soluble anti-CD3 mAb (2C11, 1 µg/mL), rMuIL6 (20 ng ml), rMuIL23 (50
496 ng/mL) and rHuTGFβ1 (0.25 ng/mL) along with neutralizing antibodies for IFN-γ (XMG1.2 clone,
497 10 µg/mL) and IL4 (11B11 clone, 10 µg ml). All antibodies and cytokines obtained from Biolegend.
498 After 5 days of *in vitro* culture, pTH17 (CD4^{+} IL-17^{eGFP+} Foxp3^{RFP-}) were FACS sorted for injection
499 into *Rag1*$^{-/-}$ mice.
500
501 **Adoptive transfer-induced colitis**: LNs and spleen were pooled from Blimp1-deficient
502 Foxp3^{RFP} IL17A^{GFP} reporter mice. CD4^{+}Foxp3^{RFP+}IL17A^{GFP-} (SP) and CD4^{+}Foxp3^{RFP+} IL17A^{GFP+}
503 (DP) cells were sorted and co-injected (1x10^{5}, i.v.) into C57BL/6 RAG1$^{-/-}$ mice along with
504 CD45RB^{hi}CD4^{+}T cells (1x10^{5}) sorted from CD45.1 mice. In some experiments,
505 CD4^{+}Foxp3^{RFP+}IL17A^{GFP-} or IL17A^{GFP+} cells or in vitro differentiated wild type IL17^{GFP+}Th17 cells
506 (5x10^{4} cells/mouse, i.p. generated as described above) were transferred in the absence of naïve
507 cells. For all experiments, recipient mice were weighed weekly. At 4-8 weeks post-transfer, mice
508 were sacrificed and colons were removed for histological analysis. Histology samples were
509 stained with H&E and scored as previously described (Read and Powrie, 2001), by a pathologist
510 in a blinded fashion.
511

512 **In vitro Treg culture**: $CD4^{+}CD25^{+}Foxp3^{GFP+}$ cells sorted from Blimp1-sufficient or deficient
513 $Foxp3^{GFP}$ reporter mice and cultured with plate coated anti-CD3 (5 µg/ml) and anti-CD28 (2.5
514 µg/ml) in the presence of rMuIL-2 (100 U/ml) and TGFβ (2 ng/ml) or rMuIL-6 (10ng/ml) plus
515 rMuIL1β (20 ng/ml) plus rMuIL23 (50 ng/ml) (all cytokines from Biolegend). Cells were cultured
516 for 3.5 days and then re-stimulated with PMA and Ionomycin for 4 hrs before analysis.

517 **Retroviral transduction:** The cording sequence of *Prdm1* was cloned into the MSCV MigR1
518 retroviral vector. $CD4^{+}Foxp3^{RFP+}$ Treg and $CD4^{+}Foxp3^{RFP-}CD44^{lo}$ naïve T cells were sorted from
519 Blimp1-deficient $Foxp3^{RFP}$ mice and activated using plate-bound anti-CD3 (5 µg/ml) and anti-
520 CD28 (2.5 µg/ml) antibodies supplemented with 100 U/ml rhIL2 (Roche) for Treg cells or with
521 rMuIL1β (20 ng/ml; Biolegend), rMuIL23 (50 ng/ml; Biolegend), rMuIL6 (10 ng/ml, Biolegend), and
522 rHuTGF-β1 (5 ng/ml; Biolegend) for Th17 cells. After 32 h of activation, cells were resuspended
523 in retrovirus-containing supernatants supplemented with 8 g/ml polybrene (Sigma-Aldrich) and
524 rhIL2 (50 U/ml) for Treg cells or IL23 (50 ng/ml) for naïve T cells, followed by centrifugation (7500
525 rpm) for 90 min at 25°C. Viral supernatant was removed and cells were re-cultured for 48 h in the
526 presence of rhIL-2 (200 U/ml) and rhTGF-β1 (10 pg/ml) for Treg cells or with media containing
527 IL1β, IL6 and TGFβ (as described above) for Th17 cells.

528

529 **Chromatin Immunoprecipitation**: $CD4^{+}Foxp3^{GFP+}$T cells were sort-purified from LN and SP
530 from Control and Blimp1CKO $Foxp3^{GFP}$ mice and stimulated with PMA and ionomycin before
531 crosslinking by fixation with 1.1 % paraformaldehyde for (10 min, RT). Sonicated chromatins
532 from 1-2x10^{6} cells were subjected to ChIP using ChIP-IT High Sensitivity kit (Active motif,
533 Carlsbad, CA). Chromatin was incubated O/N at 4°C with 5 µl of rabbit anti-Blimp1 polyclonal
534 antibody (clone 267, recognizing the C terminal of Blimp1), 5 µl of pre-immune serum, 0.8 µg of
535 anti-histone H3 (tri methyl K4) antibody (ab8580; Abcam, Cambridge, MA), 0.8 µg of anti-
536 histone H3 (tri methyl K27) antibody (07-449; Millipore, Billerica, MA), 2.5 µg of anti-RORγ

537 antibody (sc-28559; Santa Cruz Biotechnology, Dallas, TX), 2.5 μg of anti-IRF-4 antibody (sc-
538 6059; Santa Cruz Biotechnology), 2.5 μg of anti-p300 antibody (sc-585; Santa Cruz
539 Biotechnology) or 0.8 μg/2.5 μg of normal rabbit IgG (sc-2027; Santa Cruz Biotechnology), after
540 which protein G Agarose beads were added, followed by incubation at 4°C O/N. qRT-PCR was
541 performed in DNA recovered from IP and input samples [primers sequences in Supplementary
542 Table I and (Salehi et al., 2012)Analysis of sequence homology and identification of putative
543 Blimp1, *Rorc* previously confirmed binding sites, RORE consensus sites and IRF4 binding sites
544 were performed using rVista 2.0 software. Genomic sequences were obtained from Ensembl.

545

546 **Luciferase reporter assays**: A 2 kb fragment containing the *Il17a* promoter was cloned into the
547 PGL4.10 luciferase reporter plasmid (Promega, Madison, WI), with or without the CNS7 region.
548 Full length wild type Blimp1 (Blimp-Full) or a DNA-binding-lacking construct (Blimp-ΔZF) was
549 clone into pcDNA3.1(+) expression vector (Invitrogen, Waltham, MA). All primers used for
550 cloning are listed in Table SII. EL4 T cells (5×10^6) were transfected with luciferase reporter
551 plasmids (5 □g), Blimp1-expression plasmids (5 μg) and phRL-TK (2 μg) (Promega) as internal
552 control plasmid. Transfections were performed with BTX ECM830 Square Wave Electroporation
553 System (Harvard Apparatus, Holliston, MA). Total DNA amount was adjusted with the empty
554 pcDNA3.1(+) vector. Transfected cells were incubated 18 h, and then stimulated, lysed and
555 luciferase activity measured with a dual luciferase assay system (Promega).

556

557 **siRNA–mediated IRF4 knock down**: $CD4^+Foxp3^{GFP+}$ cells were sorted from Blimp-1-sufficient
558 or deficient -$Foxp3^{GFP}$ reporter mice. A mixture of three different IRF-4 specific siRNAs (100
559 pmol of each siRNA) (Integrated DNA Technologies, San Diego, CA) or scrambled control (SC)
560 siRNA (300 pmol) (Thermo Fisher Scientific, Waltham, MA) were transfected into

561 $CD4^{+}Foxp3^{GFP+}$ cells ($2x10^{6}$) by using 4D-Nucleofector System (Lonza, Basel, Switzerland) or
562 Neon Transfection system (Thermo Fisher Scientific). Transfected cells were cultured with
563 plate-boundanti-CD3 and anti-CD28. After 18 h post-transfection, cells are collected and mRNA
564 expression measured by qRTPCR. Sequences for IRF4 specific siRNAs are as previously
565 described (Staudt et al., 2010).

566

567 **Real-time quantitative PCR (qRT-PCR)**: For some experiments cells were directly FACS-sorted
568 into RLT buffer (Qiagen) supplemented with β2-mercaptoethanol.Total mRNA was isolated using
569 RNAeasy kits (Quiagen) and reverse transcribed as previously described (Salehi et al., 2012).
570 SYBR Green incorporation qRT- PCR was performed using FastStart SYBR Green Master mix
571 (Roche) in the $Realplex^{2}$ Mastercycler machine (Eppendorf). For some experiments in which cell
572 yeled was very low, Linear amplification of mRNA was performed using the MessageBooster
573 cDNA kit (Epicentre). Primers sequences for *Il17a*, *RORC*, and *BATF* are as previously described
574 (Salehi et al., 2012). All other expression primers sequences are listed in Table SI.

575

576 **Statistics**: Statistical significance was calculated by one-way ANOVA, unpaired two-tailed
577 Student's t-tests (JMP software; SAS Institute). $p \leq 0.05$ was considered significant. p values
578 denoted in figures as follows: $*$, $p < 0.05$; $**$,$p<0.01$;$***$,$p<0.001$.

579

580

581 **Author Contribution:** G.A.M. and C.O. designed all experiments. C.O., G.A.M., R.B., C.O and
582 N.H. did all experiments, collected and analyzed all data with assistance from T.N. and M.C. R.P.
583 assisted with antibiotic treatment experiment; X.F. and D.D. performed all histological analysis.

584 T.N., M.C. and S.N. provided animal breeding and genotyping technical support; C.O and G.E.
585 performed expression analysis on RORgt^{GFP}/Foxp^{RFP} reporter mice. G.A.M and C.O. wrote the
586 manuscript.

587

Acknowledgments: We are grateful to the Martins laboratory members for discussions. We thank Drs. V. Kuchroo (Harvard Medical School) and M. Fukata (CSMC) for mice and Dr. S. Targan (CSMC) for reagents. We are grateful to Drs. M. Tone, T. Araki and T. Watanabe (CSMC) for help with luciferase assays and transfection experiments and to the CSMC Flow cytometry core, especially Andres Lopez and Dr. Jo Suda for sorting.

596 **References:**

597 **Ahn, H.S., Kim, B.Y., Lim, Y.H., Lee, B.H., and Oh, K.K. (2017). Distributed Coordination for Optimal**
598 **Energy Generation and Distribution in Cyber-Physical Energy Networks. IEEE transactions on**
599 **cybernetics.**
600 **Apostolou, I., Sarukhan, A., Klein, L., and von Boehmer, H. (2002). Origin of regulatory T cells with known**
601 **specificity for antigen. Nature immunology *3*, 756-763.**
602 **Bankoti, R., Ogawa, C., Nguyen, T., Emadi, L., Couse, M., Salehi, S., Fan, X., Dhall, D., Wang, Y., Brown,**
603 **J.*, et al.* (2017). Differential regulation of Effector and Regulatory T cell function by Blimp1. Scientific**
604 **reports *7*, 12078.**
605 **Bennett, C.L., Christie, J., Ramsdell, F., Brunkow, M.E., Ferguson, P.J., Whitesell, L., Kelly, T.E., Saulsbury,**
606 **F.T., Chance, P.F., and Ochs, H.D. (2001). The immune dysregulation, polyendocrinopathy, enteropathy,**
607 **X-linked syndrome (IPEX) is caused by mutations of FOXP3. Nat Genet *27*, 20-21.**
608 **Brunkow, M.E., Jeffery, E.W., Hjerrild, K.A., Paeper, B., Clark, L.B., Yasayko, S.A., Wilkinson, J.E., Galas,**
609 **D., Ziegler, S.F., and Ramsdell, F. (2001). Disruption of a new forkhead/winged-helix protein, scurfin,**
610 **results in the fatal lymphoproliferative disorder of the scurfy mouse. Nat Genet *27*, 68-73.**
611 **Brustle, A., Heink, S., Huber, M., Rosenplanter, C., Stadelmann, C., Yu, P., Arpaia, E., Mak, T.W.,**
612 **Kamradt, T., and Lohoff, M. (2007). The development of inflammatory T(H)-17 cells requires interferon-**
613 **regulatory factor 4. Nat Immunol *8*, 958-966.**
614 **Chaudhry, A., and Rudensky, A.Y. (2013). Control of inflammation by integration of environmental cues**
615 **by regulatory T cells. The Journal of clinical investigation *123*, 939-944.**
616 **Chaudhry, A., Rudra, D., Treuting, P., Samstein, R.M., Liang, Y., Kas, A., and Rudensky, A.Y. (2009). CD4+**
617 **regulatory T cells control TH17 responses in a Stat3-dependent manner. Science *326*, 986-991.**
618 **Cimmino, L., Martins, G.A., Liao, J., Magnusdottir, E., Grunig, G., Perez, R.K., and Calame, K.L. (2008).**
619 **Blimp-1 attenuates Th1 differentiation by repression of ifng, tbx21, and bcl6 gene expression. J Immunol**
620 ***181*, 2338-2347.**
621 **Ciofani, M., Madar, A., Galan, C., Sellars, M., Mace, K., Pauli, F., Agarwal, A., Huang, W., Parkurst, C.N.,**
622 **Muratet, M.*, et al.* (2012). A validated regulatory network for Th17 cell specification. Cell *151*, 289-303.**
623 **Cretney, E., Xin, A., Shi, W., Minnich, M., Masson, F., Miasari, M., Belz, G.T., Smyth, G.K., Busslinger, M.,**
624 **Nutt, S.L.*, et al.* (2011). The transcription factors Blimp-1 and IRF4 jointly control the differentiation and**
625 **function of effector regulatory T cells. Nat Immunol *12*, 304-311.**
626 **Crotty, S., Johnston, R.J., and Schoenberger, S.P. (2010). Effectors and memories: Bcl-6 and Blimp-1 in T**
627 **and B lymphocyte differentiation. Nat Immunol *11*, 114-120.**
628 **Dias, S., D'Amico, A., Cretney, E., Liao, Y., Tellier, J., Bruggeman, C., Almeida, F.F., Leahy, J., Belz, G.T.,**
629 **Smyth, G.K.*, et al.* (2017). Effector Regulatory T Cell Differentiation and Immune Homeostasis Depend**
630 **on the Transcription Factor Myb. Immunity *46*, 78-91.**
631 **Fontenot, J.D., Rasmussen, J.P., Williams, L.M., Dooley, J.L., Farr, A.G., and Rudensky, A.Y. (2005).**
632 **Regulatory T cell lineage specification by the forkhead transcription factor foxp3. Immunity *22*, 329-**
633 **341.**
634 **Heinemann, C., Heink, S., Petermann, F., Vasanthakumar, A., Rothhammer, V., Doorduijn, E.,**
635 **Mitsdoerffer, M., Sie, C., Prazeres da Costa, O., Buch, T.*, et al.* (2014). IL-27 and IL-12 oppose pro-**
636 **inflammatory IL-23 in CD4+ T cells by inducing Blimp1. Nature communications *5*, 3770.**
637 **Ichiyama, K., Yoshida, H., Wakabayashi, Y., Chinen, T., Saeki, K., Nakaya, M., Takaesu, G., Hori, S.,**
638 **Yoshimura, A., and Kobayashi, T. (2008). Foxp3 inhibits RORgammat-mediated IL-17A mRNA**
639 **transcription through direct interaction with RORgammat. The Journal of biological chemistry *283*,**
640 **17003-17008.**

641 **Iwasaki, Y., Fujio, K., Okamura, T., Yanai, A., Sumitomo, S., Shoda, H., Tamura, T., Yoshida, H., Charnay,**
642 **P., and Yamamoto, K. (2013). Egr-2 transcription factor is required for Blimp-1-mediated IL-10**
643 **production in IL-27-stimulated CD4+ T cells. European journal of immunology *43*, 1063-1073.**
644 **Jain, R., Chen, Y., Kanno, Y., Joyce-Shaikh, B., Vahedi, G., Hirahara, K., Blumenschein, W.M., Sukumar,**
645 **S., Haines, C.J., Sadekova, S.*, et al.* (2016). Interleukin-23-Induced Transcription Factor Blimp-1**
646 **Promotes Pathogenicity of T Helper 17 Cells. Immunity *44*, 131-142.**
647 **Johnston, R.J., Poholek, A.C., DiToro, D., Yusuf, I., Eto, D., Barnett, B., Dent, A.L., Craft, J., and Crotty, S.**
648 **(2009). Bcl6 and Blimp-1 are reciprocal and antagonistic regulators of T follicular helper cell**
649 **differentiation. Science *325*, 1006-1010.**
650 **Josefowicz, S.Z., Lu, L.F., and Rudensky, A.Y. (2012). Regulatory T cells: mechanisms of differentiation**
651 **and function. Annu Rev Immunol *30*, 531-564.**
652 **Kim, B., and Belza, B. (2017). Toward an Equitable Society for Every Generation. Journal of**
653 **gerontological nursing *43*, 2-4.**
654 **Kim, B.S., Lu, H., Ichiyama, K., Chen, X., Zhang, Y.B., Mistry, N.A., Tanaka, K., Lee, Y.H., Nurieva, R.,**
655 **Zhang, L.*, et al.* (2017). Generation of RORgammat(+) Antigen-Specific T Regulatory 17 Cells from**
656 **Foxp3(+) Precursors in Autoimmunity. Cell reports *21*, 195-207.**
657 **Kim, J.M., Rasmussen, J.P., and Rudensky, A.Y. (2007). Regulatory T cells prevent catastrophic**
658 **autoimmunity throughout the lifespan of mice. Nat Immunol *8*, 191-197.**
659 **Kim, S.J., Zou, Y.R., Goldstein, J., Reizis, B., and Diamond, B. (2011). Tolerogenic function of Blimp-1 in**
660 **dendritic cells. The Journal of experimental medicine *208*, 2193-2199.**
661 **Levine, A.G., Medoza, A., Hemmers, S., Moltedo, B., Niec, R.E., Schizas, M., Hoyos, B.E., Putintseva, E.V.,**
662 **Chaudhry, A., Dikiy, S.*, et al.* (2017). Stability and function of regulatory T cells expressing the**
663 **transcription factor T-bet. Nature *546*, 421-425.**
664 **Linterman, M.A., Pierson, W., Lee, S.K., Kallies, A., Kawamoto, S., Rayner, T.F., Srivastava, M., Divekar,**
665 **D.P., Beaton, L., Hogan, J.J.*, et al.* (2011). Foxp3+ follicular regulatory T cells control the germinal center**
666 **response. Nature medicine *17*, 975-982.**
667 **Lochner, M., Peduto, L., Cherrier, M., Sawa, S., Langa, F., Varona, R., Riethmacher, D., Si-Tahar, M., Di**
668 **Santo, J.P., and Eberl, G. (2008). In vivo equilibrium of proinflammatory IL-17+ and regulatory IL-10+**
669 **Foxp3+ RORgamma t+ T cells. The Journal of experimental medicine *205*, 1381-1393.**
670 **Martins, G., and Calame, K. (2008). Regulation and functions of Blimp-1 in T and B lymphocytes. Annu**
671 **Rev Immunol *26*, 133-169.**
672 **Martins, G.A., Cimmino, L., Liao, J., Magnusdottir, E., and Calame, K. (2008). Blimp-1 directly represses**
673 **Il2 and the Il2 activator Fos, attenuating T cell proliferation and survival. The Journal of experimental**
674 **medicine *205*, 1959-1965.**
675 **Martins, G.A., Cimmino, L., Shapiro-Shelef, M., Szabolcs, M., Herron, A., Magnusdottir, E., and Calame,**
676 **K. (2006). Transcriptional repressor Blimp-1 regulates T cell homeostasis and function. Nat Immunol *7*,**
677 **457-465.**
678 **Montes de Oca, M., Kumar, R., de Labastida Rivera, F., Amante, F.H., Sheel, M., Faleiro, R.J., Bunn, P.T.,**
679 **Best, S.E., Beattie, L., Ng, S.S.*, et al.* (2016). Blimp-1-Dependent IL-10 Production by Tr1 Cells Regulates**
680 **TNF-Mediated Tissue Pathology. PLoS pathogens *12*, e1005398.**
681 **Neumann, C., Heinrich, F., Neumann, K., Junghans, V., Mashreghi, M.F., Ahlers, J., Janke, M., Rudolph,**
682 **C., Mockel-Tenbrinck, N., Kuhl, A.A.*, et al.* (2014). Role of Blimp-1 in programing Th effector cells into**
683 **IL-10 producers. The Journal of experimental medicine *211*, 1807-1819.**
684 **Ohnmacht, C. (2016). Tolerance to the Intestinal Microbiota Mediated by ROR(gammat)(+) Cells. Trends**
685 **in immunology *37*, 477-486.**
686 **Ohnmacht, C., Park, J.H., Cording, S., Wing, J.B., Atarashi, K., Obata, Y., Gaboriau-Routhiau, V., Marques,**
687 **R., Dulauroy, S., Fedoseeva, M.*, et al.* (2015). MUCOSAL IMMUNOLOGY. The microbiota regulates type**
688 **2 immunity through RORgammat(+) T cells. Science *349*, 989-993.**

689 **Parish, I.A., Marshall, H.D., Staron, M.M., Lang, P.A., Brustle, A., Chen, J.H., Cui, W., Tsui, Y.C., Perry, C.,**
690 **Laidlaw, B.J.*, et al.* (2014). Chronic viral infection promotes sustained Th1-derived immunoregulatory**
691 **IL-10 via BLIMP-1. The Journal of clinical investigation *124*, 3455-3468.**
692 **Read, S., and Powrie, F. (2001). Induction of inflammatory bowel disease in immunodeficient mice by**
693 **depletion of regulatory T cells. Current protocols in immunology / edited by John E Coligan [et al]**
694 ***Chapter 15*, Unit 15 13.**
695 **Robertson, E.J., Charatsi, I., Joyner, C.J., Koonce, C.H., Morgan, M., Islam, A., Paterson, C., Lejsek, E.,**
696 **Arnold, S.J., Kallies, A.*, et al.* (2007). Blimp1 regulates development of the posterior forelimb, caudal**
697 **pharyngeal arches, heart and sensory vibrissae in mice. Development *134*, 4335-4345.**
698 **Rubtsov, Y.P., Rasmussen, J.P., Chi, E.Y., Fontenot, J., Castelli, L., Ye, X., Treuting, P., Siewe, L., Roers, A.,**
699 **Henderson, W.R., Jr.*, et al.* (2008). Regulatory T cell-derived interleukin-10 limits inflammation at**
700 **environmental interfaces. Immunity *28*, 546-558.**
701 **Salehi, S., Bankoti, R., Benevides, L., Willen, J., Couse, M., Silva, J.S., Dhall, D., Meffre, E., Targan, S., and**
702 **Martins, G.A. (2012). B Lymphocyte-Induced Maturation Protein-1 Contributes to Intestinal Mucosa**
703 **Homeostasis by Limiting the Number of IL-17-Producing CD4+ T Cells. Journal of immunology *189*, 5682-**
704 **5693.**
705 **Sefik, E., Geva-Zatorsky, N., Oh, S., Konnikova, L., Zemmour, D., McGuire, A.M., Burzyn, D., Ortiz-Lopez,**
706 **A., Lobera, M., Yang, J.*, et al.* (2015). MUCOSAL IMMUNOLOGY. Individual intestinal symbionts induce**
707 **a distinct population of RORgamma(+) regulatory T cells. Science *349*, 993-997.**
708 **Staudt, V., Bothur, E., Klein, M., Lingnau, K., Reuter, S., Grebe, N., Gerlitzki, B., Hoffmann, M., Ulges, A.,**
709 **Taube, C.*, et al.* (2010). Interferon-regulatory factor 4 is essential for the developmental program of T**
710 **helper 9 cells. Immunity *33*, 192-202.**
711 **Ward-Hartstonge, K.A., McCall, J.L., McCulloch, T.R., Kamps, A.K., Girardin, A., Cretney, E., Munro, F.M.,**
712 **and Kemp, R.A. (2017). Inclusion of BLIMP-1(+) effector regulatory T cells improves the Immunoscore in**
713 **a cohort of New Zealand colorectal cancer patients: a pilot study. Cancer immunology, immunotherapy**
714 **: CII *66*, 515-522.**
715 **Wei, G., Wei, L., Zhu, J., Zang, C., Hu-Li, J., Yao, Z., Cui, K., Kanno, Y., Roh, T.Y., Watford, W.T.*, et al.***
716 **(2009). Global mapping of H3K4me3 and H3K27me3 reveals specificity and plasticity in lineage fate**
717 **determination of differentiating CD4+ T cells. Immunity *30*, 155-167.**
718 **Wheaton, J.D., Yeh, C.H., and Ciofani, M. (2017). Cutting Edge: c-Maf Is Required for Regulatory T Cells**
719 **To Adopt RORgammat(+) and Follicular Phenotypes. J Immunol *199*, 3931-3936.**
720 **Wohlfert, E.A., Grainger, J.R., Bouladoux, N., Konkel, J.E., Oldenhove, G., Ribeiro, C.H., Hall, J.A., Yagi,**
721 **R., Naik, S., Bhairavabhotla, R.*, et al.* (2011). GATA3 controls Foxp3(+) regulatory T cell fate during**
722 **inflammation in mice. The Journal of clinical investigation *121*, 4503-4515.**
723 **Xu, M., Pokrovskii, M., Ding, Y., Yi, R., Au, C., Harrison, O.J., Galan, C., Belkaid, Y., Bonneau, R., and**
724 **Littman, D.R. (2018). c-MAF-dependent regulatory T cells mediate immunological tolerance to a gut**
725 **pathobiont. Nature *554*, 373-377.**
726 **Yamanaka, S., Tajiri, S., Fujimoto, T., Matsumoto, K., Fukunaga, S., Kim, B.S., Okano, H.J., and Yokoo, T.**
727 **(2017). Generation of interspecies limited chimeric nephrons using a conditional nephron progenitor**
728 **cell replacement system. Nature communications *8*, 1719.**
729 **Zheng, Y., Chaudhry, A., Kas, A., deRoos, P., Kim, J.M., Chu, T.T., Corcoran, L., Treuting, P., Klein, U., and**
730 **Rudensky, A.Y. (2009). Regulatory T-cell suppressor program co-opts transcription factor IRF4 to control**
731 **T(H)2 responses. Nature *458*, 351-356.**
732 **Zheng, Y., Josefowicz, S.Z., Kas, A., Chu, T.T., Gavin, M.A., and Rudensky, A.Y. (2007). Genome-wide**
733 **analysis of Foxp3 target genes in developing and mature regulatory T cells. Nature *445*, 936-940.**
734 **Zhou, L., and Littman, D.R. (2009). Transcriptional regulatory networks in Th17 cell differentiation.**
735 **Current opinion in immunology *21*, 146-152.**

Zhou, L., Lopes, J.E., Chong, M.M., Ivanov, II, Min, R., Victora, G.D., Shen, Y., Du, J., Rubtsov, Y.P., Rudensky, A.Y.*, et al.* (2008). TGF-beta-induced Foxp3 inhibits T(H)17 cell differentiation by antagonizing RORgammat function. Nature *453*, 236-240.

Figure legends:

Figure 1: Blimp1 is preferentially expressed in microbiome specific RORγt$^+$Foxp3$^+$Treg cells and it is required to repress IL17A expression.

(**A**) Blimp1^{YFP} expression in RORγt$^+$Helios$^-$ (purple) and RORγt$^-$Helios$^+$ (black) Foxp3$^+$ Treg subsets cells (FACS plot, left and histograms, middle) and frequency of RORγt$^+$ cells in Foxp3$^+$Blimp1^{YFP+} and Foxp3$^+$Blimp1^{YFP-} cells (bar graph, right) in the large intestines lamina propria (LI-LP) and mesenteric lymph nodes (MLN) from Blimp1^{YFP} reporter mice.

(**B**) *Prdm1* (Blimp1) mRNA expression (qPCR) in Foxp3$^+$RORγt$^+$ and Foxp3$^+$RORγt$^-$ cells sorted from the lamina propria of the small intestine from RORγt^{GFP}Foxp3^{RFP} dual reporter mice. Data shown is expression of *Prdm1* mRNA relative to the mean of two housekeeping genes of indicated populations form two independent experiments.

(**C**) IL17A expression in splenic CD4$^+$Foxp3$^+$RORγt$^+$ cells from *Prdm1*$^{+/+}$Foxp3$^{CREYFP+}$ and *Prdm1*$^{F/F}$Foxp3$^{CREYFP+}$ mice (FACS plot, left and cumulative bar graph, right).

(**D**) IL17A expression in CD4$^+$Foxp3$^+$RORγt$^+$IRF4$^+$ cells (top plots; bar color indicate intensity of IL17 expression); and representative histograms showing expression of RORγt (top left) or IRF4 (bottom left) in Blimp1-sufficient (blue) or sufficient (red) Foxp3$^+$ cells. Bar graphs (right side) show average MFI of RORγt (top right) or IRF4 (bottom right) in Blimp1-sufficient or sufficient Foxp3$^+$ cells.

(**E**) IL17A (top) and IL10 (middle) expression in Blimp1-sufficient (CRE$^-$) and Blimp1-deficient (CRE$^+$) TCRβ$^+$CD4$^+$Foxp3$^+$ cells from the same mice (PRDM1$^{F/F}$Foxp3$^{CREYFP+}$ female mice). Representative FACS plots showing gating of CRE$^+$ and CRE$^-$ cells in the MLN (top) and Spleen (SP; bottom) and bar graphs showing frequency of IL17A$^+$ (left) and IL10$^+$ (right) cells.

765 (**F**) Expression of *Prdm1*, *Il17a*, *Rorc* and *Foxp3* mRNA (qRT-PCR, relative to β2microglobulin)
766 in $CD4^{+}Foxp3^{+}$ cells sorted from $Prdm1^{F/F}$ and $Prdm1^{+/+}Foxp3^{CREYFP+}$ mice and re-stimulated in
767 vitro.
768 (**G**) Expression of IL17A in $TCR\beta^{+}CD4^{+}Fxop3^{+}$ cells from the MLN from antibiotic treated (VNAM)
769 or non-treated (NT) $Prdm1^{F/F}CD4^{CRE+}$ mice.
770
771 Data is representative of at least two independent experiments; bars show average and error
772 bars, SEM ($n \geqq 3$, per group); each symbol represents one mouse. *p<0.05 and **p<0.01,
773 unpaired student's *t* test (**A**, **C**, **D**, **F** and **G**), paired student's *t* test (**E**).
774
775
776
777 **Figure 2: Binding of Blimp1 to the *Il17a/Il17f* locus in $Foxp3^{+}$ Treg cells is associated with**
778 **decreased locus accessibility**.
779 **(A)** Representative FACS plots (top) and bar graph showing IL17A expression in gated GFP^{+}
780 Blimp1-deficient $Foxp3^{+}$ Treg cells transduced with MIG-R1 or Blimp1-expressing MIG-R1
781 retrovirus (MIG-R1Blimp1) (plots) and Blimp1-deficient in vitro-differentiated Th17 cells (bar
782 graphs).
783 (**B**) ChIP assays in $CD4^{+}Foxp3^{GFP+}$ Treg cells (sorted from Blimp1-sufficient $Foxp3^{GFP}$ reporter
784 mice) and *in vitro* differentiated pTh17 cells showing binding of Blimp1 to different regions of the
785 *Il17a/Il17f* locus. NG, negative control (non-relate gene lacking Blimp1 binding sites); NR, non-
786 relate region in the *Il17a/Il17f* locus lacking Blimp1 binding sites. Top schematic illustrates the
787 location of sites evaluated in **B**-**D**. *Il17a* and *Il17f* genes are represented by arrows indicating the
788 transcription direction; promoter regions, black ovals and CNS regions grey ovals.
789 **(C)** ChIP assays showing enrichment of H3K4me3 (black bars) and H3K27me3 (grey bars) at
790 different regions of the *Il17a/Il17f* locus in blimp1-suffcient (Control; Ctrl) or Blimp1-deficient
791 (CKO) $CD4^{+}Foxp3^{GFP+}$Treg cells (empty bars show results from Ctrl antibody IP).

792 **(D)** ChIP assays showing enrichment of p300 at the *Il17a* promoter and *Il17* CNS7 regions in
793 $CD4^{+}Foxp3^{GFP+}$Treg cells sorted from Ctrl and CKO mice and in wild type pTh17 cells.
794 **(E)** Representation of promoter constructs (top) and luciferase activity assay (bottom) showing
795 increased activity of the *Il17a* promoter in the presence of the CNS7 region containing a Blimp1
796 binding site and its inhibition by co-transfection of full length but not truncated Blimp1 constructs.
797 Striped bars, control plasmid; black bars, Blimp1-full length; grey bars, truncated Blimp1, lacking
798 the zinc finger-containing region.
799 Data shown is from two (A) or three independent experiments (B-E); error bars, SEM ($n \geqq 3$, per
800 group). *$p<0.05$ and **$p<0.01$, one-way ANOVA.
801

802 **Figure 3: Increased binding of IRF4 at the *Il17* locus and IRF4 requirement for IL17A**

803 **production in Blimp1-deficient Foxp3^{+}Treg cells.**

804 (**A**) Schematic representation (upper) of the *Il17a/Il17f* locus indicating RORγt and IRF4 binding

805 sites evaluated in ChIP assays (shown in **A** and **C**), and RORγt ChIP assay (lower) in Blimp1-

806 sufficient or deficient CD4^{+}Foxp3^{GFP+}Treg cells compared to *in vitro* differentiated wild type

807 pTh17 cells.

808 (**B**) IL17A expression (top FACS plots and bar graph) in TCRβ^{+}CD4^{+}Foxp3^{+}Treg cells from the

809 MLN from *Prdm1*$^{+/+}$*Rorc*$^{+/+}$Foxp3$^{CREYFP+}$ (Control, Ctrl), *Prdm1*$^{F/F}$*Rorc*$^{+/+}$Foxp3$^{CREYFP+}$ (KO) and

810 *Prdm1*$^{F/F}$*Rorc*$^{F/F}$Foxp3$^{CREYFP+}$ mice and expression of *Foxp3*, *Prdm1*, *Rorc* and *Il17a* mRNA

811 (qRT-PCR, relative to β2microglobulin) (bottom graphs) in sorted and *in vitro* stimulated (PMA

812 and ionomycin for 4hr) CD4^{+}Foxp3$^{CREYFP+}$ cells.

813 (**C**) ChIP assay showing binding of IRF4 at the *Il17a/Il17f* CNS7 and *Il10* Intron I regions in

814 Blimp1-sufficient and deficient CD4^{+}Foxp3^{GFP+}Treg cells compared to *in vitro* differentiated wild

815 type pTh17 cells.

816 (**D**) Evaluation of *IRF4, Il17a* and *Il10* mRNA expression following IRF4 knockdown. Expression

817 levels (relative to β2Microglobulin) were determined by qRT-PCR using total RNA from Ctrl and

818 CKO Foxp3^{+}Treg cells 18 h after transfection with IRF4 siRNA or negative control (SC) siRNA.

819 (N=1mice/group; data shown is from one experiment; similar results were obtained in two

820 additional independent experiments).

821

822 Data shown in **A**-**C** is representative from at least two independent experiments. Error bars,

823 SEM ($n \geqq 3$, per group). *p<0.05 and **p<0.01, one-way ANOVA.

824

825 **Figure 4: IL17A-producing Blimp1-deficient Foxp3^{+}Treg cells fail to suppress intestinal**
826 **inflammation.**

827 (**A**) Body weight of Rag$^{-/-}$ mice adoptively transferred with allotype-marked (CD45.1) naïve
828 (CD45RB^{low}) CD4^{+}T cells alone or in combination with Blimp-1-deficient IL17A-producing
829 (IL17^{+}Treg) or non-producing (IL17A^{-}Treg) Foxp3^{+} Treg cells.

830 (**B**) Colon length in mice shown in (A) and analyzed 8 weeks' post adoptive cell transfer.

831 (**C**) Colon histological sections (Hematoxylin-eosin-stained; 10x magnification) from mice shown
832 in A-B, 8 weeks after cell transfer.

833 (**D**) Frequency (FACS plots, left) of IL17^{GFP+} cells in CD45.1^{+} Treg cells and absolute numbers
834 (bar graphs, right) of naïve CD4^{+}T cells (CD45.1^{+} cells) recovered from the colonic lamina
835 propria from mice show in A-C.

836 (**E**) Frequency cumulative of IL17A^{GFP+} cells in Treg cells recovered from the LI-LP, MLN and
837 SP from mice show in A-D.

838 (**F**) IL17A expression (ELISA) in the supernatants of total LI-LP cells stimulated with PMA and
839 ionomycin for 4hr.

840

841 Data shown is from one experiment. Error bars, SEM (N=3-4 mice/ group). *p<0.05 and
842 **p<0.01, one-way ANOVA (**A**, **B**, **D** and **F**) and unpaired student's t test (**E**).

843

844 **Supplementary Table I.** Primers sequences used for gene expression analysis.

Gene/Site	Primer Sequence (5'-3')
B2M FWR	GCTCGCGCTACTCTCTCTTT
B2M REV	TCTGAATGCTCCACTTTTTCAA
PRDM1 FWR	TTGAGATTGCTTGTGCTGCT
PRDM1 REV	TCTCCAACCTGAAGGTCCAC
Il10 FWR	AGCTGGACAACATACTGC
Il10 REV	CTTGTAGACACCTTGGGTC
Il17f FWR	CAAAACCAGGGCATTTCTGT
Il17f REV	ATGGTGCTGTCTTCCTGACC
SOCS2 FWR	TACCGGTACGATCTGGGGACTGC
SOCS2 REV	AGGGCCTCTGGGTTCTCTTTC
CCR5 FWR	CATCCGTTCCCCCTACAAGA
CCR5 REV	GGAACTGACCCTTGAAAATCCA
IRF4 FWR	GCCCAACAAGCTAGAAAG
IRF4 REV	TCTCTGAGGGTCTGGAAACT
Foxp3 FWR	CAGCTGCAGCTGCCTACA
Foxp3 REV	GATCCCAGGTGGCAGGC

845

846 **Supplementary Table II.** Primers sequences used for ChIP.

Gene/Site	Primer Sequence (5'-3')
SNAIL/NG FWR	ATTGCCGTCCCAGAGAAGGAT
SNAIL/NG REV	TACACAGATATGGCCATTTGCC
Il17a/Il17f CNS2 FWR	TGTGGTTGTCTAAGCCATGC
Il17a/Il17f CNS2 REV	CAGCAACTGACTGGGTTTCA

Il17a-3.3 Kb FWR	GCCTCCCATGTGGTCATTAT
Il17a-3.3 Kb REV	AGGCTCCTTCTCCATTGGTT
Il17a intron I FWR	CTCATCACAATGAGTTTGTCA
Il17a intron I REV	AGGCTCAGCAGCAGCAAC
Il17a/Il17f CNS7 FWR	CTGAGTTGGGGGCTGTGTAT
Il17a/Il17f CNS7 REV	CATATCGAGGGTGTCGGACT
Il17a Promoter FWR	GTAGTCTCCACCCGGCAGT
Il17a Promoter REV	TTTGAGGTTCGGTATCAAGC
Il17a/f NR FWR	ACCCCAGATCCAAGGAGACT
Il17a/f NR REV	CCTAAGCATGCACCTGTGTG
Rorc-1 FWR	CACAGCGTGTGGTTTGGTTT
Rorc-1 REV	GCGCATGCAAATTCTTTGAC
Rorc-2 FWR	TATCGGTCCACCTCATGCTG
Rorc-2 REV	ACTGCCGGGTGGAGACTACT
Rorc-3 FWR	ATGGCTGCTTCTTCCCTCAG
Rorc-3 REV	CCTTTGATTCCCCTTCAGGA
Rorc-5 FWR	CTTTCTTTCATCTGTTTGAGATAGG
Rorc-5 REV	CCAGGCAGCTGATGAAGATA
Rorc-6 FWR	TTGTTGCTGCTTGGGTATGC
Rorc-6 REV	TGCTTTAAGGGCCACCATTT
Il10 Inrton I FWR	GCAAAAATAGCTCTCCTTCTCC
Il10 Intron I REV	GGATGTGCCTGGGTTTAGTT

847

848

849

850 **Supplementary Table III.** Primers sequences used for cloning.

Primer name	Primer Sequence (5'-3')
*Il17a*pro-F	ACATAGCTCGAGAACAGACAGCCACATACCAAA
*Il17a*pro-R	CAGTCTAAGCTTGTGGATGAAGAGTAGTGCTCCT
*Il17*CNS7-F	ACATAGGGTACCTATAGCCTGCAGCCCTGCA
*Il17*CNS7-R	CAGTCTGAGCTCGGTGTCGGACTTTACATTAGCAGAC
Blimp-F	ACATAGGAATTCATGAGAGAGGCTTATCTCAGATGTTG
Blimp-R	ACATAGCTCGAGTTAAGGATCCATCGGTTCAACTG
Blimp-ZFdel-R	ACATAGCTCGAGTTACTGTTTCTTCAGAGGGTAAGGAAGAG

851

Figure 1

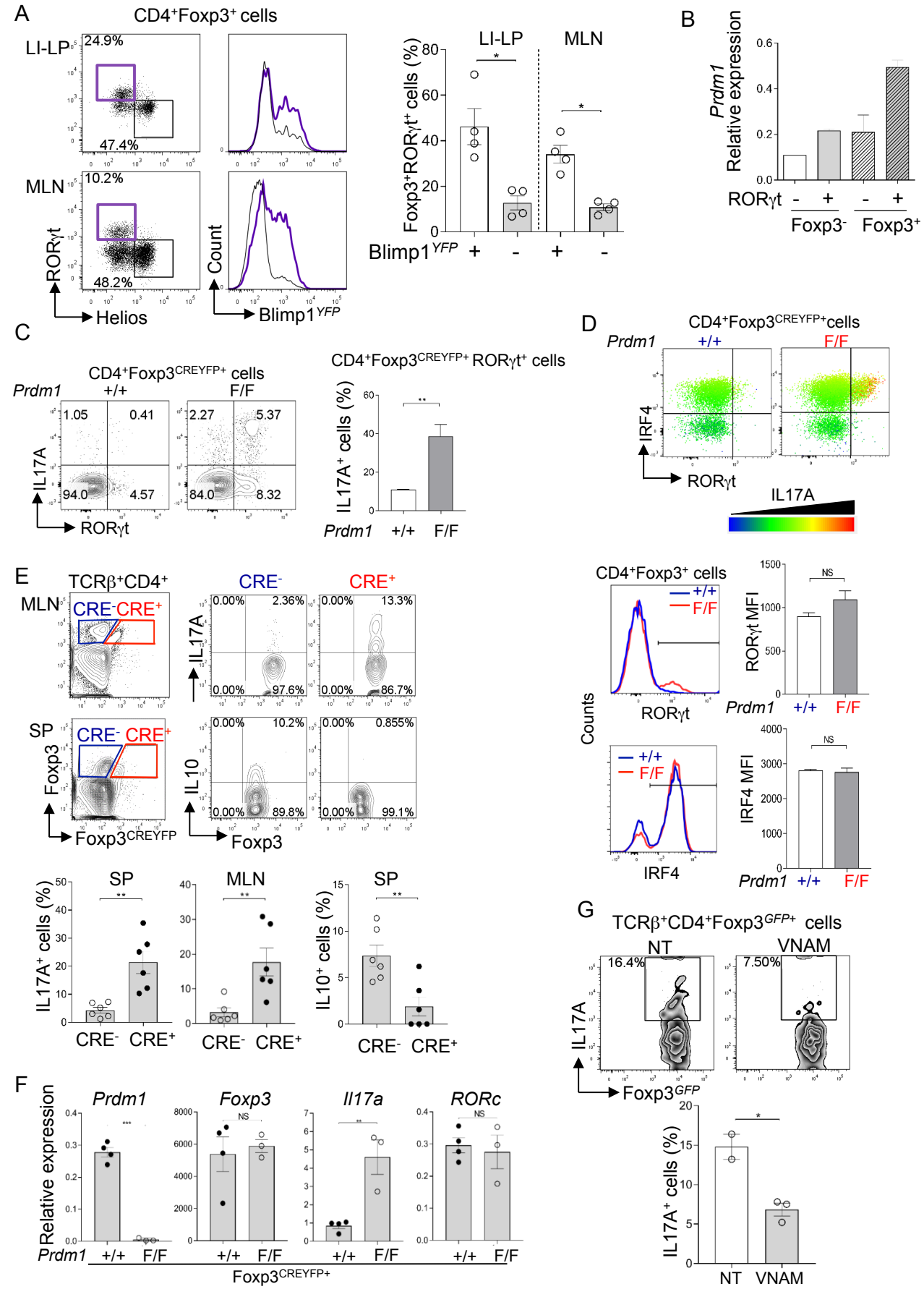
A
CD4+Foxp3+ cells
LI-LP
24.9%
47.4%
MLN
10.2%
48.2%
RORγt
Helios
Count
Blimp1YFP
LI-LP
MLN
Foxp3+RORγt+ cells (%)
Blimp1YFP + - + -
B
Prdm1 Relative expression
RORγt - + - +
Foxp3- Foxp3+
C
CD4+Foxp3CREYFP+ cells
Prdm1 +/+ F/F
1.05 0.41 94.0 4.57
2.27 5.37 84.0 8.32
IL17A
RORγt
CD4+Foxp3CREYFP+ RORγt+ cells
IL17A+ cells (%)
Prdm1 +/+ F/F
D
CD4+Foxp3CREYFP+cells
Prdm1 +/+ F/F
IRF4
RORγt
IL17A
E
TCRβ+CD4+
MLN
CRE- CRE+
SP
Foxp3
Foxp3CREYFP
CRE- CRE+
0.00% 2.36% 0.00% 97.6%
0.00% 13.3% 0.00% 86.7%
IL17A
0.00% 10.2% 0.00% 89.8%
0.00% 0.855% 0.00% 99.1%
IL10
Foxp3
SP
MLN
SP
IL17A+ cells (%)
IL10+ cells (%)
CRE- CRE+
CD4+Foxp3+ cells
+/+
F/F
Counts
RORγt
RORγt MFI
NS
Prdm1 +/+ F/F
IRF4
IRF4 MFI
G
TCRβ+CD4+Foxp3GFP+ cells
NT
VNAM
16.4%
7.50%
IL17A
Foxp3GFP
IL17A+ cells (%)
NT VNAM
F
Prdm1
Foxp3
Il17a
RORc
Relative expression
NS
Prdm1 +/+ F/F
Foxp3CREYFP+

Figure 2

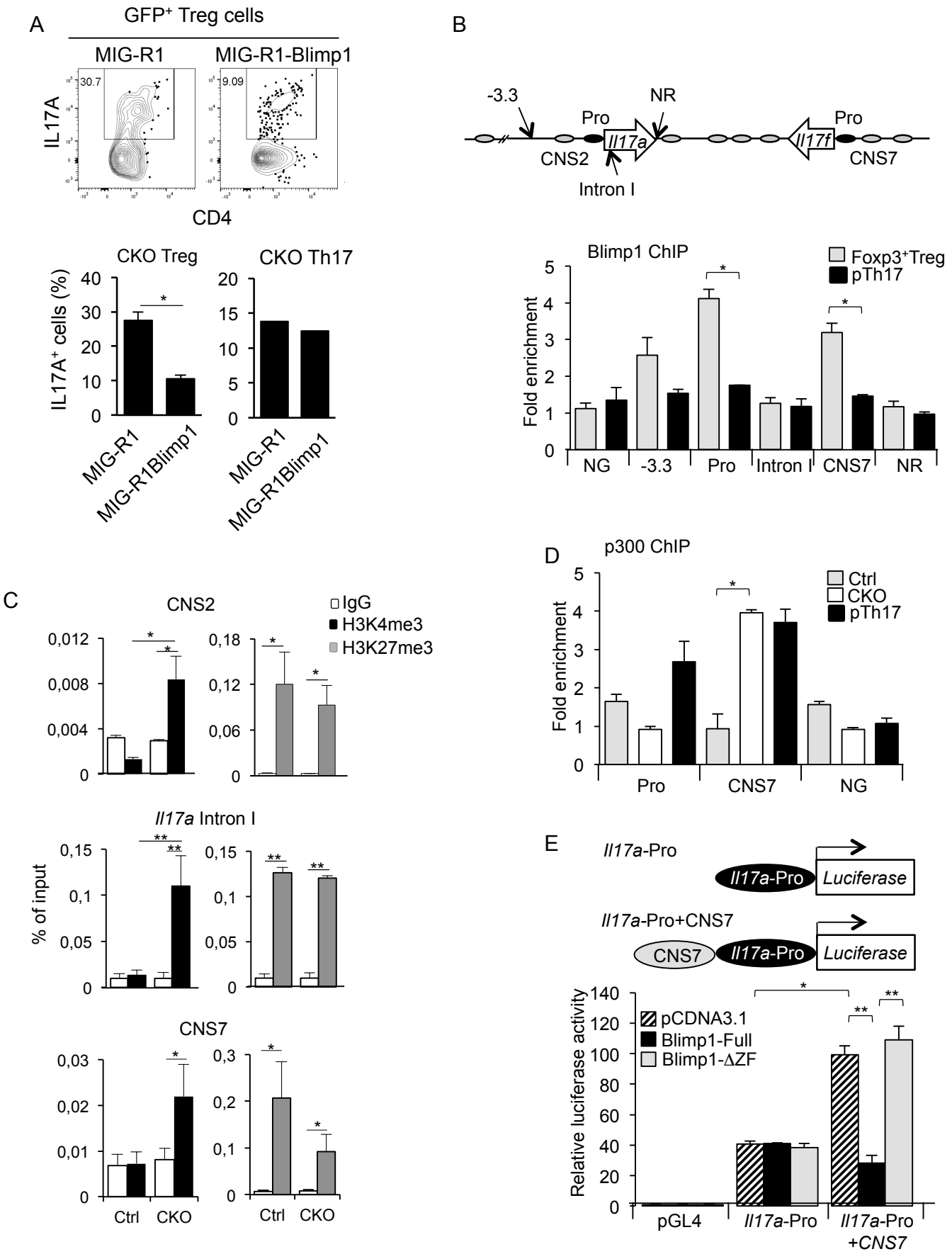
A
GFP+ Treg cells
MIG-R1
MIG-R1-Blimp1
30.7
9.09
IL17A
CD4
CKO Treg
CKO Th17
IL17A+ cells (%)
MIG-R1
MIG-R1Blimp1
B
-3.3
NR
Pro
Il17a
Il17f
CNS2
CNS7
Intron I
Blimp1 ChIP
Foxp3+Treg
pTh17
Fold enrichment
NG
-3.3
Pro
Intron I
CNS7
NR
C
CNS2
IgG
H3K4me3
H3K27me3
Il17a Intron I
% of input
CNS7
Ctrl
CKO
D
p300 ChIP
Ctrl
CKO
pTh17
Fold enrichment
Pro
CNS7
NG
E
Il17a-Pro
Luciferase
Il17a-Pro+CNS7
CNS7
Relative luciferase activity
pCDNA3.1
Blimp1-Full
Blimp1-ΔZF
pGL4
Il17a-Pro
Il17a-Pro +CNS7

Figure 3

A

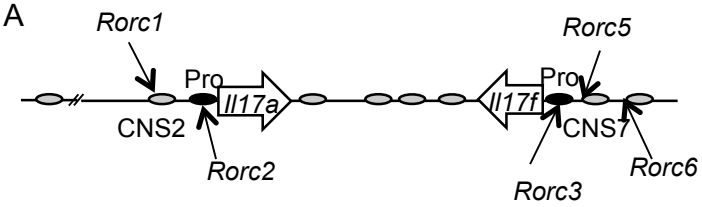

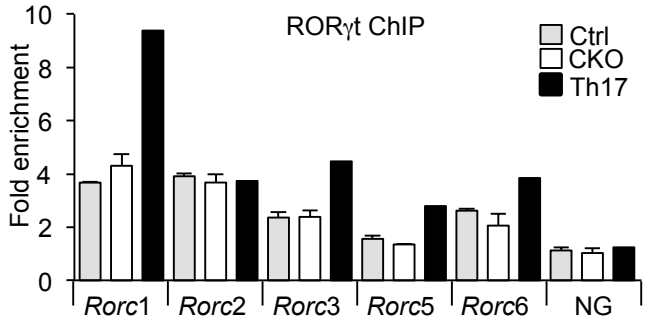

B

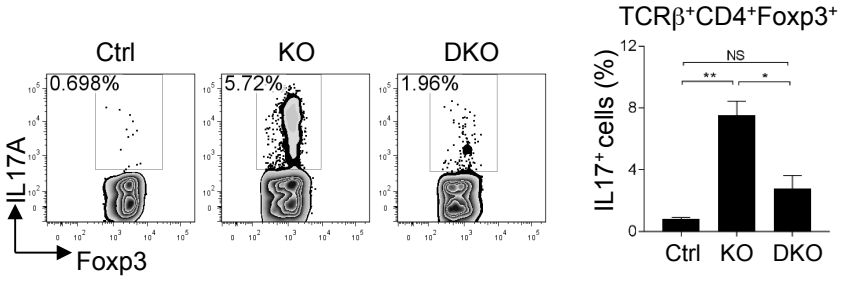

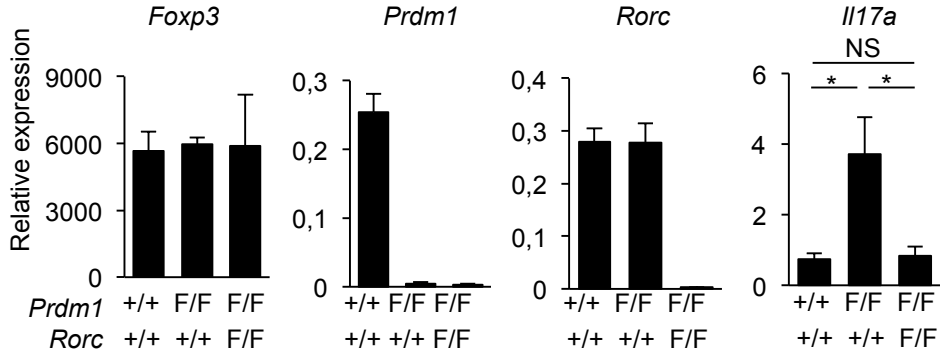

C

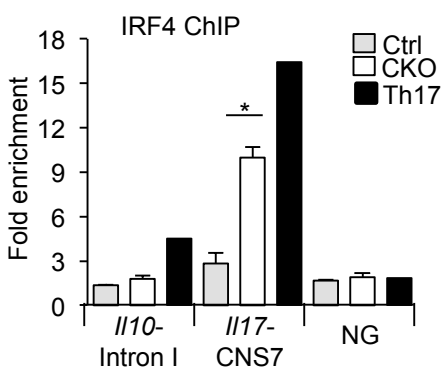

D

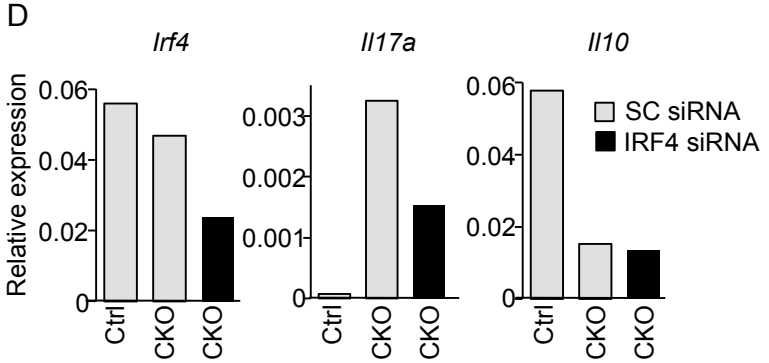

Figure 4

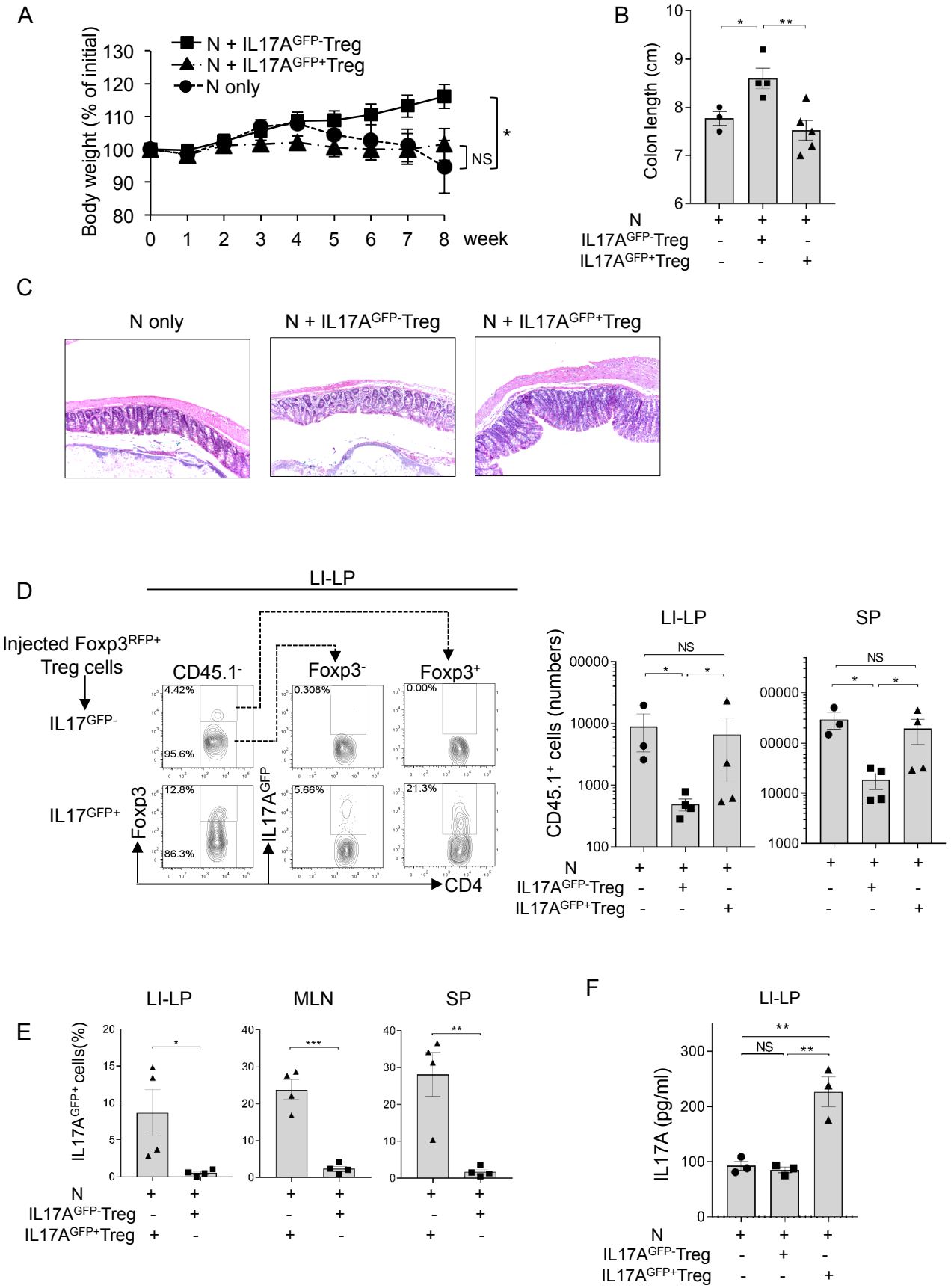
A
Body weight (% of initial)
N + IL17A^GFP-Treg
N + IL17A^GFP+Treg
N only
NS
*
week
B
Colon length (cm)
N
IL17A^GFP-Treg
IL17A^GFP+Treg
C
N only
N + IL17A^GFP-Treg
N + IL17A^GFP+Treg
D
LI-LP
Injected Foxp3^RFP+ Treg cells
IL17^GFP-
IL17^GFP+
CD45.1-
Foxp3-
Foxp3+
4.42%
95.6%
0.308%
0.00%
12.8%
86.3%
5.66%
21.3%
Foxp3
IL17A^GFP
CD4
LI-LP
SP
CD45.1+ cells (numbers)
NS
N
IL17A^GFP-Treg
IL17A^GFP+Treg
E
LI-LP
MLN
SP
IL17A^GFP+ cells(%)
N
IL17A^GFP-Treg
IL17A^GFP+Treg
F
LI-LP
IL17A (pg/ml)
NS
N
IL17A^GFP-Treg
IL17A^GFP+Treg

Supplemental Figure 1

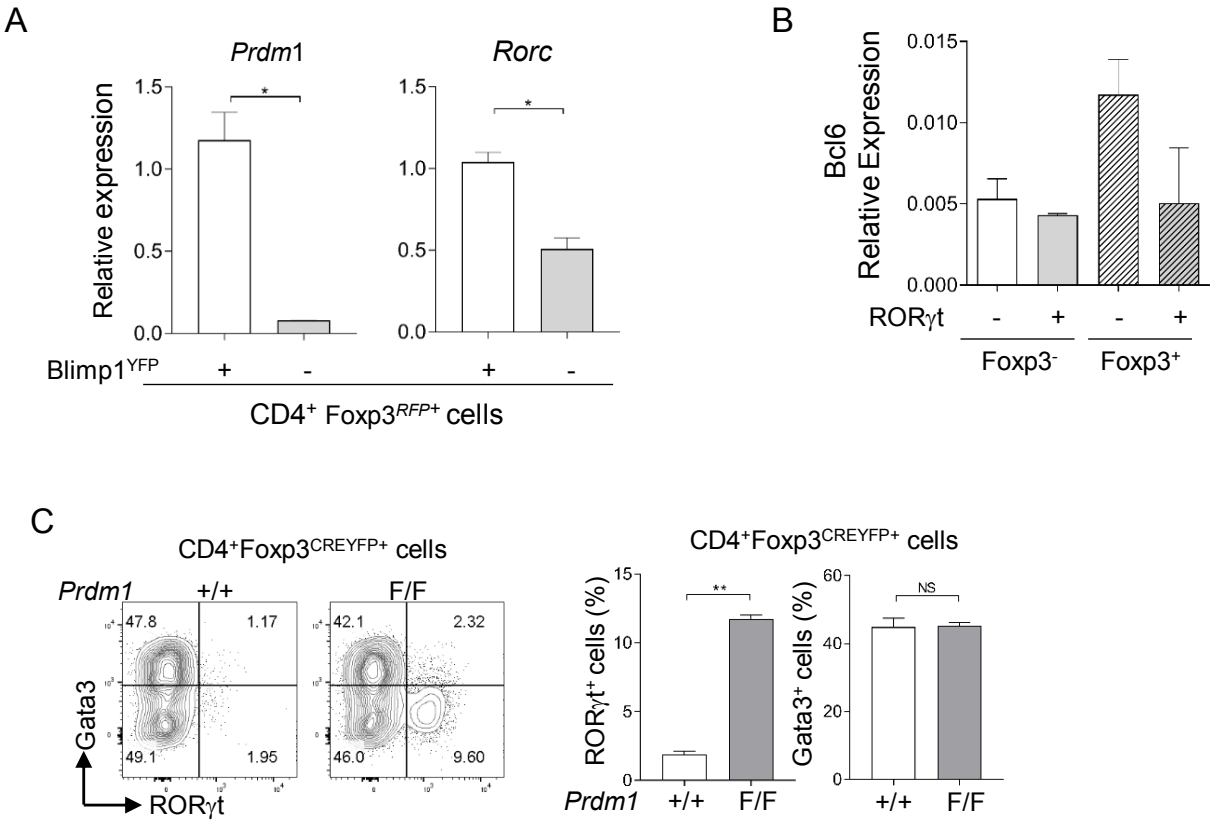

Supplemental Figure 1: Blimp1 expression in RORγt⁺Foxp3⁺Treg cells. (**A**) *Prdm1* and *Rorc* mRNA expression (qRT-PCR, relative to β2microglobulin) in CD4⁺Foxp3^{RFP+}Blimp1^{YFP-} and CD4⁺Foxp3^{RFP+}Blimp1^{YFP+} cells sorted from Blimp1^{YFP}Foxp3^{RFP} dual reporter mice. (**B**) *Bcl6* mRNA expression (qRT-PCR) in same cells shown in Fig. 1B. (**C**) Frequency of RORγt⁺ and GATA3⁺ cells in CD4⁺Foxp3$^{CREYFP+}$ cells from the mesenteric lymph nodes from *Prdm1*$^{+/+}$Foxp3$^{CREYFP+}$ or *Prdm1*$^{F/F}$Foxp3$^{CREYFP+}$ mice. Data shown is from at least two independent experiments. Bars show average and error bars, SEM (N ≧ 3 mice/group). *p<0.05 and **p<0.01, unpaired student's t test.

Supplemental Figure 2

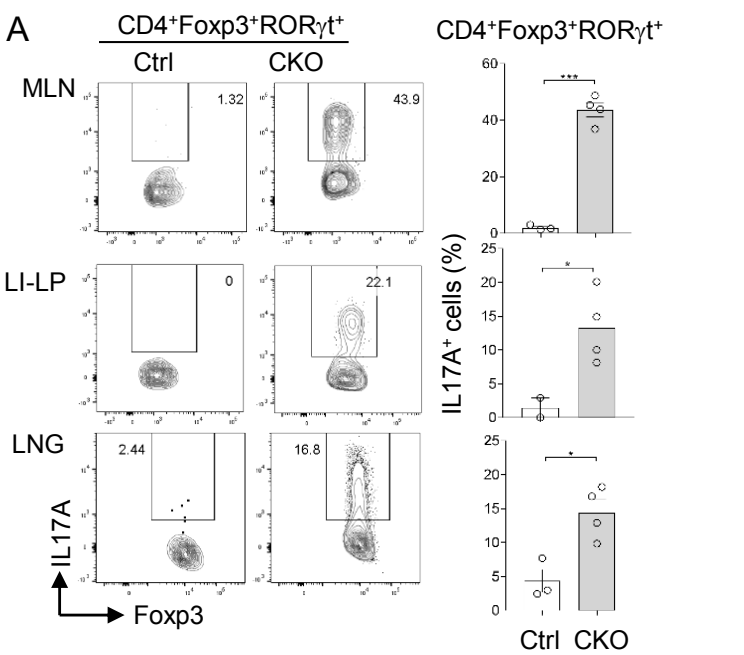

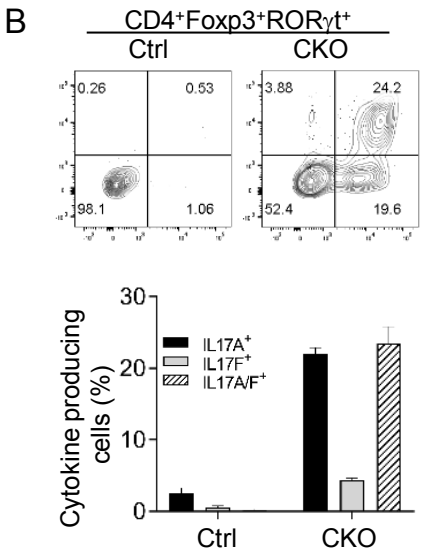

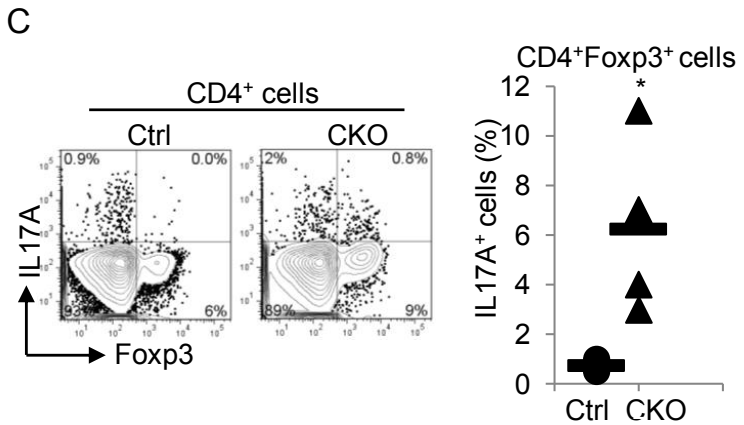

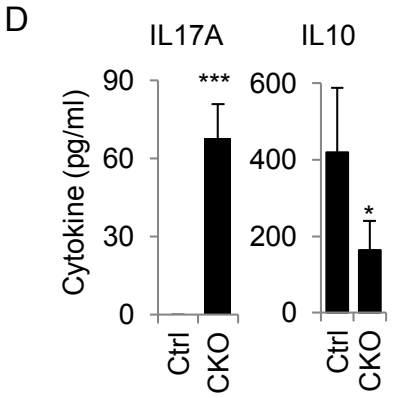

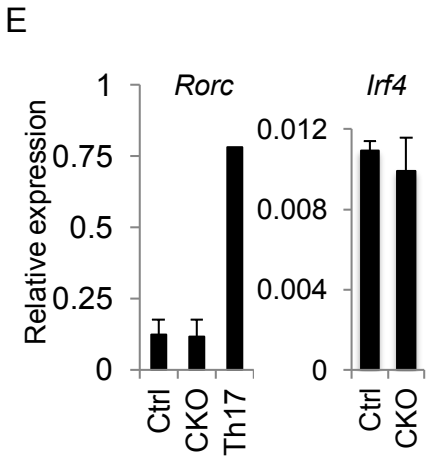

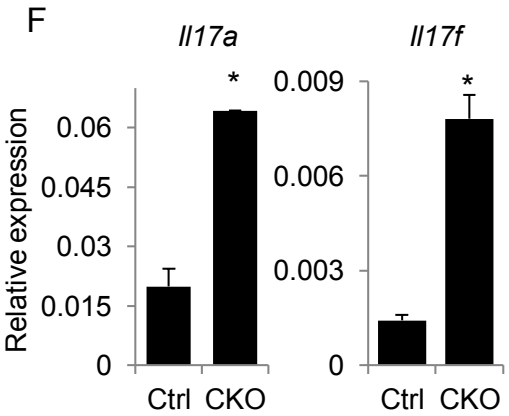

Supplemental Figure 2: Requirement of Blimp1 to suppress IL17 expression in Foxp3^{+}RORγt^{+}Treg cells. (**A**) Representative Facs plots (left) and cumulative data (graphs, right) showing the frequency of IL17A^{+} cells in CD4^{+}Foxp3^{+}RORγt^{+} cells from the mesenteric lymph nodes (MLN), colonic intestinal lamina propria (LI-LP) and lungs (LNG) from Ctrl or *Prdm1*$^{F/F}$CD4^{CRE+} (CKO) mice. Cells were stimulated by PMA and ionomycin for 4 h with addition of Brefeldin A for the last 2 h before intracellular cytokine staining. (**B**) Expression of IL17A and IL17F in CD4^{+}Foxp3^{+}RORγt^{+} cells from the MLN of Ctrl and *Prdm1*$^{F/F}$CD4^{CRE+}Foxp3^{GFP} (CKO) mice. Cells were stimulated as in (**A**) before staining. (**C**) Expression of IL17A and Foxp3 protein in cells from the MLN of Ctrl or *Prdm1*$^{F/F}$CD4^{CRE+} (CKO) mice. Cells were stimulated as in (**A**) before staining. (**D**) IL17A and IL10 expression (ELISA) in supernatants of CD4^{+}Foxp3^{GFP+} cells sort purified from Ctrl or *Prdm1*$^{F/F}$CD4^{CRE+}Foxp3^{GFP} mice and stimulated with anti-CD3 and CD28 for 18 h. (**E**) *Irf4* and *Rorc* mRNA expression (qRT-PCR, relative to β2microglobulin) in CD4^{+}Foxp3^{GFP+} cells sorted from Ctrl and *Prdm1*$^{F/F}$CD4^{CRE+}Foxp3^{GFP} (CKO) mice. (**F**) *Il17a* and *Il17f* mRNA expression (qRT-PCR) in CD4^{+}Foxp3^{GFP+} cells sorted from SP and MLN from Ctrl and *Prdm1*$^{F/F}$CD4^{CRE+}Foxp3^{GFP} (CKO) mice and stimulated *in vitro* with anti-CD3 and CD28 for 24 h. Data shown is from at least two independent experiments. Bars show average and error bars, SEM (N ≧ 3 mice/group). *$p<0.05$ and ***$p<0.001$, unpaired student's t test.

Supplemental Figure 3

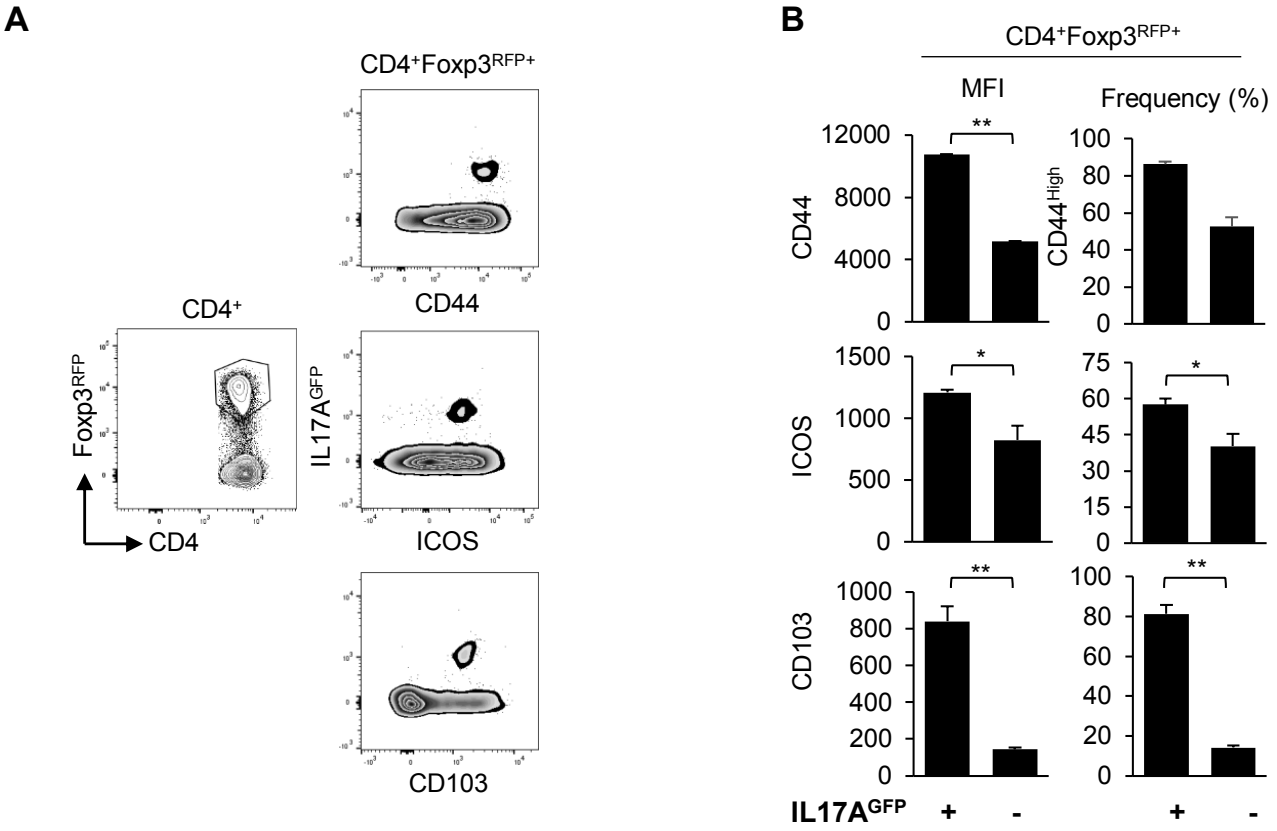

Supplemental Figure 3: increased expression of effector molecules in IL17 producing Blimp1-deficient RORγt⁺ Treg cells. Left panel: (A) Representative FACS plots of IL17A^{GFP} and effector molecules (CD44, ICOS and CD103) expression in CD4^{+}Foxp3^{RFP+}Treg cells from the spleen from *Prdm1*$^{F/F}$CD4^{CRE+}Foxp3^{RFP}IL17A^{GFP} mice. (**B**) Cumulative expression data (MFI and frequency) of same molecules as in A, in IL17A^{GFP+} and IL17A^{GFP-} CD4^{+}Foxp3^{RFP+}Treg cells. Bars (**B**) show average and error bars, SEM (N = 3 mice). **p*<0.05 and ***p*<0.01, paired student's *t* test.

Supplemental Figure 4

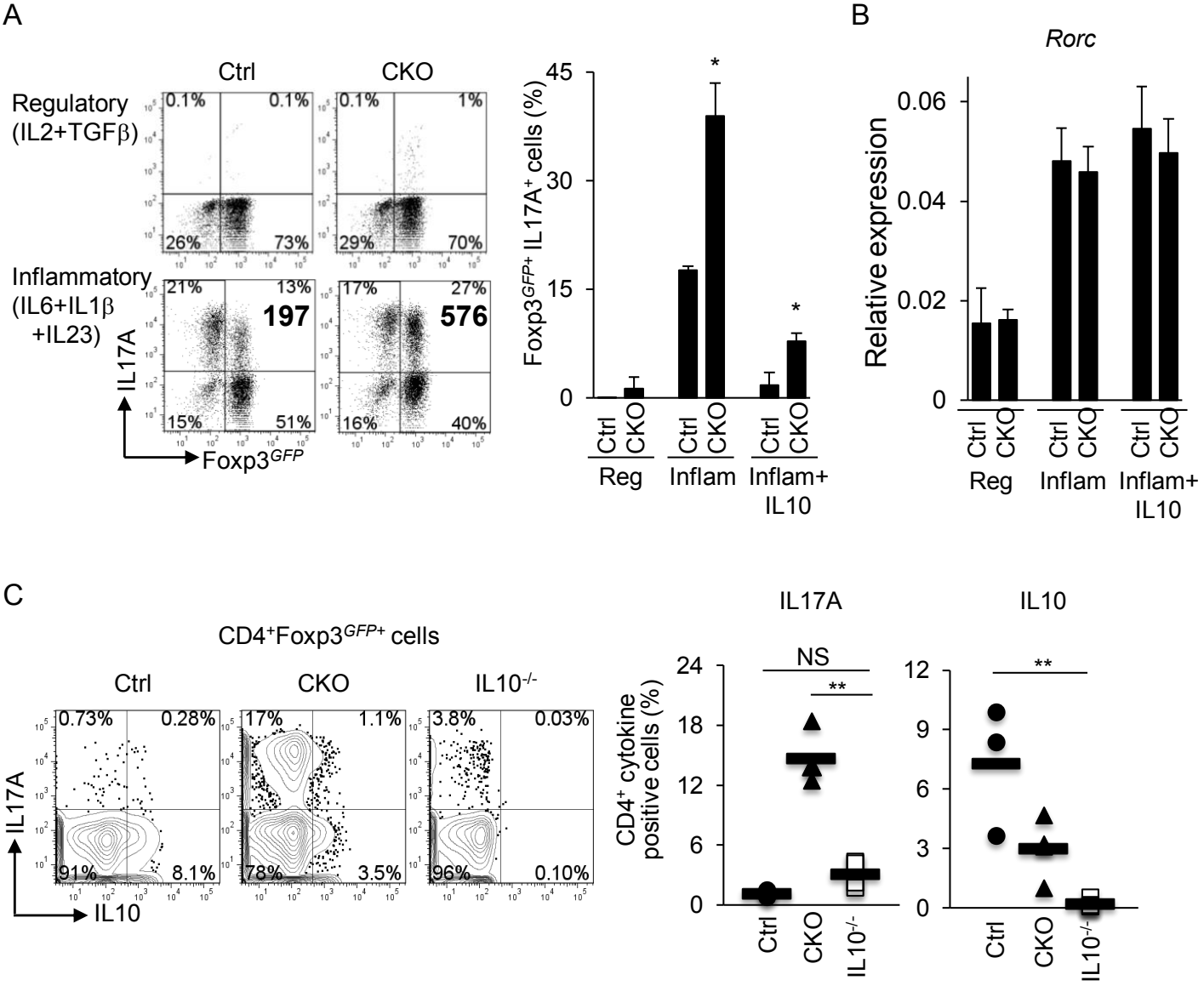

Supplemental Figure 4: Expression of IL17 by Blimp1-deficient Foxp3⁺ Treg cells is not secondary to impaired IL10 expression. (**A**) FACS plots (left) showing expression of IL17A and Foxp3^{GFP} in sorted CD4^{+}Foxp3^{GFP+} cells from *Prdm1*$^{+/+}$CD4^{CRE+} (Ctrl) and *Prdm11*$^{F/F}$CD4^{CRE+} (CKO) mice. Sorted cells were in the presence of IL2 and TGFβ, (regulatory conditions; top plots), or IL6, IL1b and IL23 (inflammatory conditions; bottom plots) or inflammatory condition plus rMuIL10 for 5 days and then re-stimulated for 6 hours (anti-CD3 and CD28). Bar graph (right) shows frequency of IL17A^{+} cells in CD4^{+}Foxp3^{GFP+} cells. Numbers in bold in FACS plots are MFI of IL17A staining. (**B**) *Rorc* mRNA expression (qRT-PCR, relative to β2microglobulin) in same cells shown in (**A**). (**C**) FACS plots (left) and scatter plots (right) showing expression of IL17A and IL10 in splenic CD4^{+}Foxp3^{GFP+} cells from Blimp1-suffcient (Ctrl), Blimp1-deficient (CKO) and Blimp1-sufficient Il10$^{-/-}$ mice (IL10$^{-/-}$). Data shown is representative from at least two independent experiments. Bars show average and error bars, SEM (N ≧ 3 mice/group). *p<0.05, **p<0.01, unpaired student's t test (**A** and **B**), one-way ANOVA (**C**).

Supplemental Figure 5

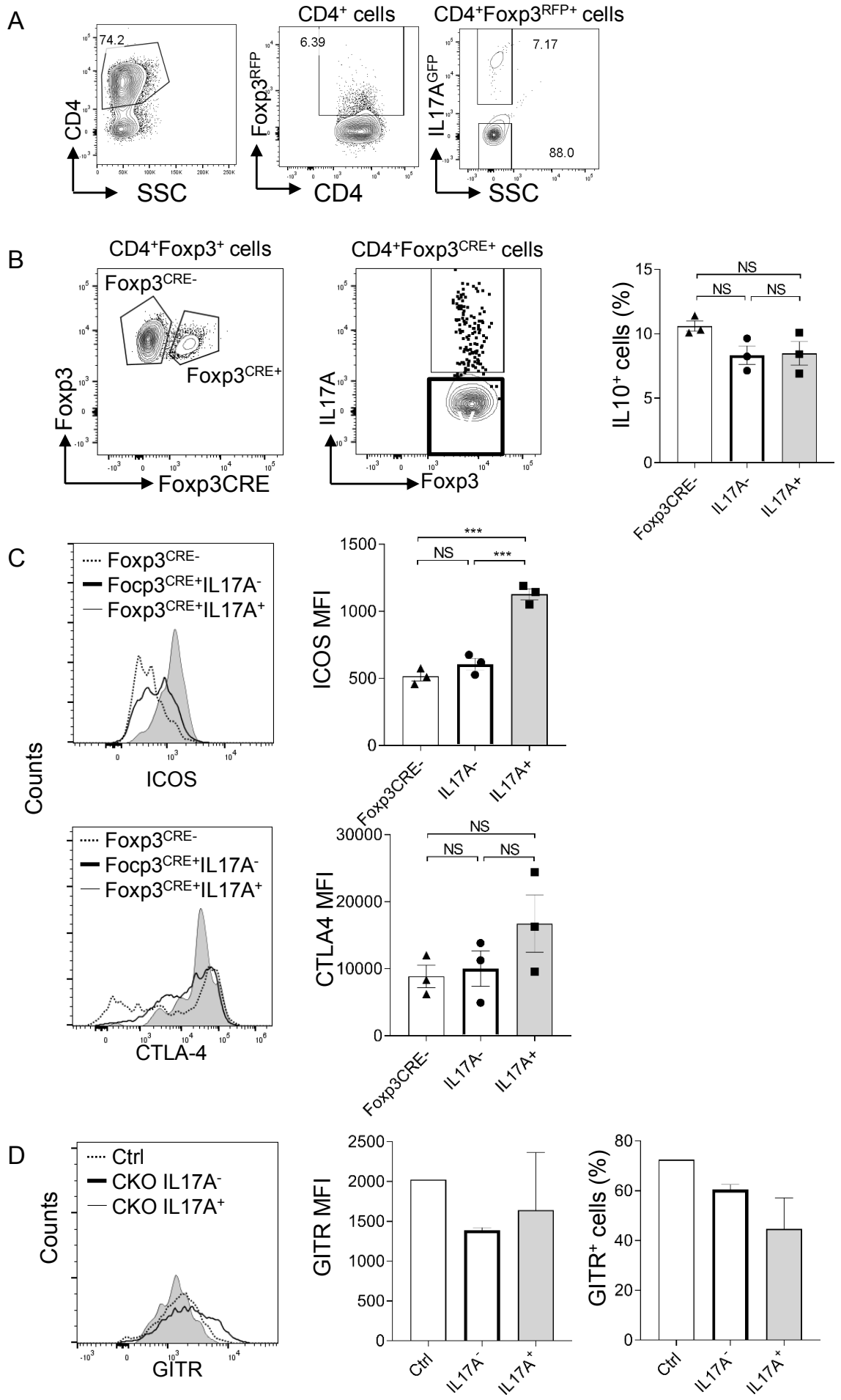

Supplemental Figure 5: Expression of Treg effector molecules does not segregate with IL17A expression in Blimp1-deficient Foxp3^{+} Treg cells. (**A**) FACS plots showing gating strategy for sorting of IL17AGFP^{+} and IL17AGFPCD4^{+}Foxp3RFP^{+} cells from *Prdm1*$^{F/F}$CD4^{CRE+}Foxp3^{RFP}IL17A^{GFP} mice. (**B**) IL10 expression in Blimp1-sufficient (CRE-) and Blimp1-deficient (CRE+) in IL17A^{GFP+} and IL17A^{GFP-} Foxp3^{+} Treg cells from Prdm1$^{F/F}$ Foxp3^{CRE+} female mice. (**C**) Expression (median intensity fluorescence, MFI) of ICOS and CTLA-4 in the same cells shown in (**B**). (**D**) Expression (MFI, left and frequency, right) of GITR in Blimp1-sufficient, and Blimp1-deficient Foxp3^{+}IL17A^{+} and Foxp3^{+}IL17A^{-} cells from *Prdm1*$^{F/F}$CD4^{CRE+} mice. Bars show average and error bars, SEM (N ≧ 3 mice/group). ***p<0.001, one-way ANOVA (**B** and **C**).

Supplemental Figure 6

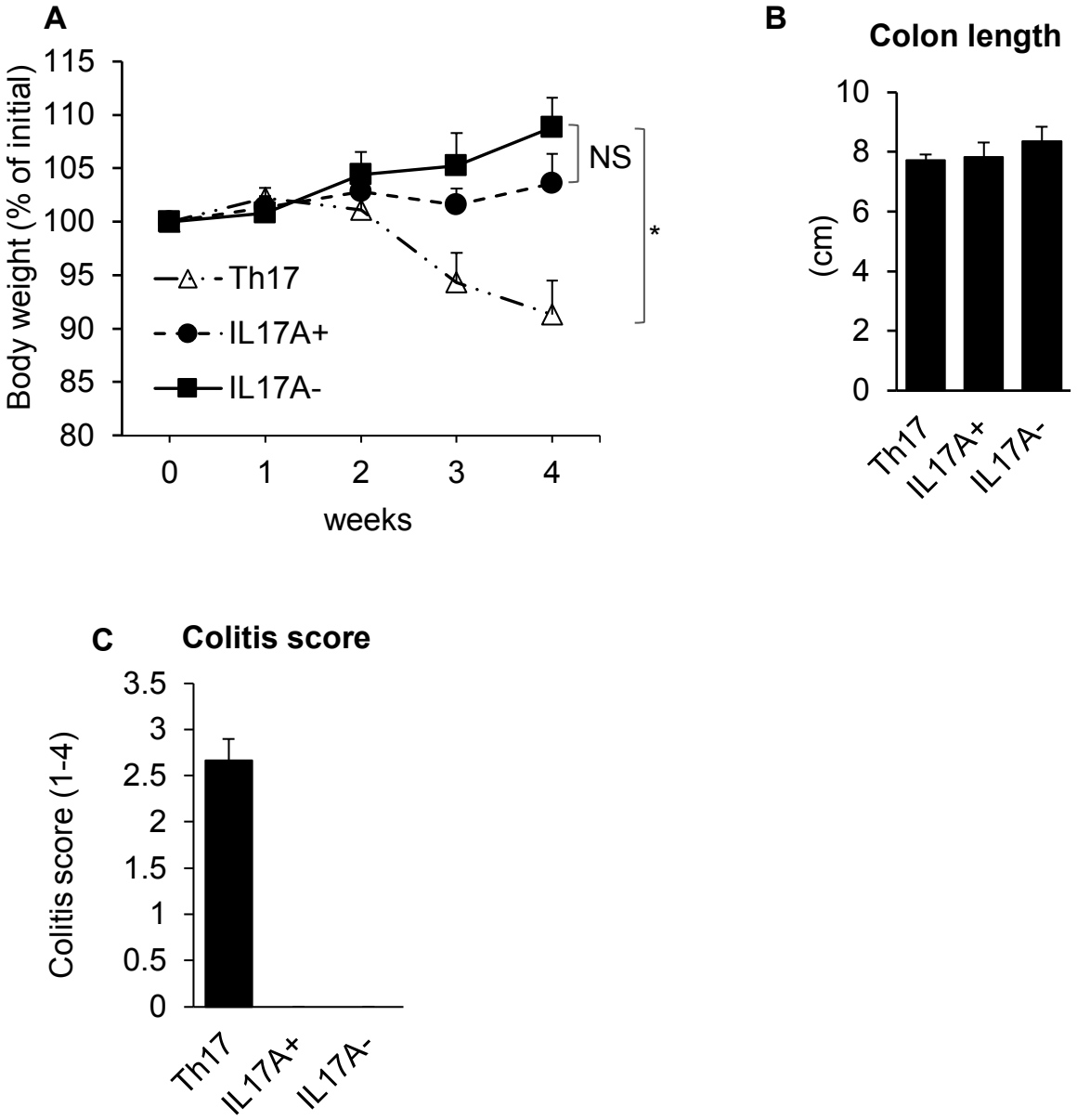

Supplemental figure 6: IL17A-producing Blimp1-deficient Foxp3^{+}Treg cells are not sufficient to cause intestinal inflammation.

(**A**) Body weight of Rag$^{-/-}$ mice adoptively transferred with in vitro differentiate wild type Th17 cells (Th17), Blimp-1-deficient IL17A-producing (IL17^{+}Treg) or non-producing (IL17A^{-}Treg) Foxp3^{+} Treg cells.

(**B**) Colon length in mice shown in (A) and analyzed 4 weeks' post adoptive cell transfer.

(**C**) Colon histological scores from mice shown in A-B, 4 weeks after cell transfer.

Data shown is from one experiment. Error bars, SEM (N=2-6mice/ group). *p<0.05 and **p<0.01, one-way ANOVA (**A**, **B**, **D** and **F**) and unpaired student's t test (**E**). Similar data was obtained on a separated experiment.

Supplemental Figure 7

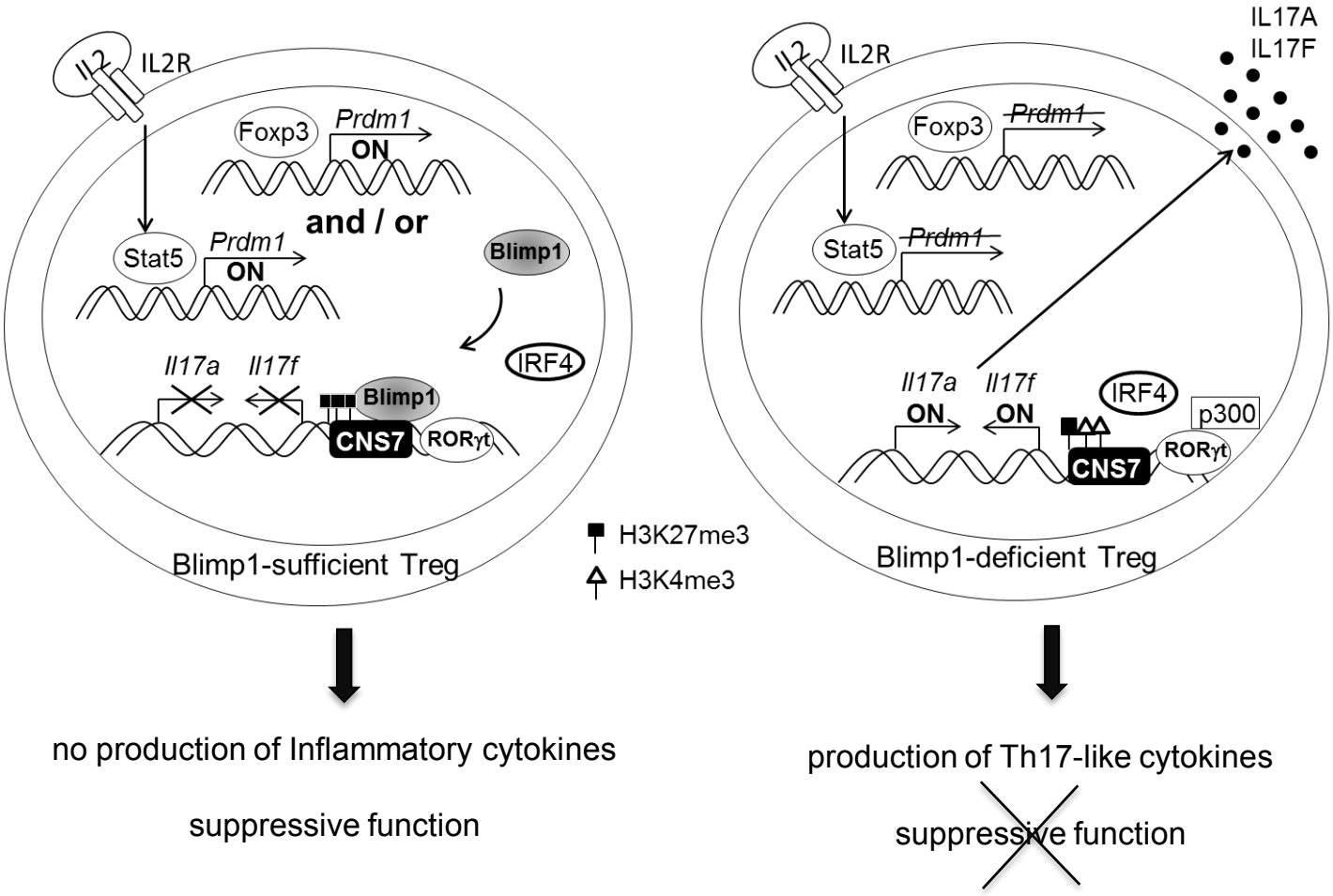

Supplemental Figure 7: A model for Blimp1-mediate repression of the *Il17a/f* locus in Foxp3⁺ Treg cells. Constitutive expression of Blimp1 in effector Foxp3⁺ Treg cells is likely induced downstream of Foxp3 and/or IL2 signaling. Binding of Blimp1 to the CNS7 region of the *Il17a/f* locus prevents binding of IRF4 and thus impedes RORγt-mediate transcription of *Il17 (*left*).* Lack of Blimp1 (right) results in increased locus accessibility, associated with decreased amounts of H3K27me3, and increased levels of H3K4me3 and p300 binding to the locus. The increased locus accessibility would favor IRF4 binding, which in turn facilitates *Il17* transcription by RORγt.